Journal of Controlled Release 286 (2018) 326–347

Contents lists available at ScienceDirect

Journal of Controlled Release

journal homepage: www.elsevier.com/locate/jconrel

Single-chain polymer nanoparticles in controlled drug delivery and targeted imaging

A. Pia P. Kröger[a], Jos M.J. Paulusse[a,b,*]

[a] Department of Biomolecular Nanotechnology, MESA+ Institute for Nanotechnology and TechMed Institute for Health and Biomedical Technologies, Faculty of Science and Technology, University of Twente, P.O. Box 217, 7500 AE Enschede, The Netherlands
[b] Department of Nuclear Medicine and Molecular Imaging, University Medical Center Groningen, P.O. Box 30.001, 9700 RB, Groningen, The Netherlands

ARTICLE INFO

Keywords:
Single chain polymer nanoparticles
Intramolecular cross-linking
Biomedical applications
Targeted imaging
Controlled drug delivery

ABSTRACT

As a relatively new class of materials, single-chain polymer nanoparticles (SCNPs) just entered the field of (biomedical) applications, with recent advances in polymer science enabling the formation of bio-inspired nanosized architectures. Exclusive intramolecular collapse of individual polymer chains results in individual nanoparticles. With sizes an order of magnitude smaller than conventional polymer nanoparticles, SCNPs are in the size regime of many proteins and viruses (1–20 nm). Multifaceted syntheses and design strategies give access to a wide set of highly modular SCNP materials. This review describes how SCNPs have been rendered water-soluble and highlights ongoing research efforts towards biocompatible SCNPs with tunable properties for controlled drug delivery, targeted imaging and protein mimicry.

1. Introduction

Polymer nanoparticles based on individual polymer chains, coined Single-Chain Polymer Nanoparticles (SCNPs) have been developed over the past two decades [1–4]. SCNPs are accomplished by exclusive intramolecularly collapsing/folding of the polymer, which leads to exceptionally small polymer nanoparticles in the sub-20 nm size range. The collapse is either achieved by self-assembly or by covalent cross-linking of functional groups on the precursor polymer or rather mediated by external cross-linkers [1]. SCNPs have been prepared via multiple ways, including via irreversible and dynamic covalent cross-linking reactions such as thermal cycloaddition [5, 6], Cu(I)-mediated click chemistry [7–9], olefin metathesis [10], disulfide [11] and hydrazone [12] formation as well as via non-covalent cross-linking interactions, including hydrogen-bonding motifs and metal coordination, which have been comprehensively reviewed earlier [1–4, 13–18]. Whereas SCNP formation was originally carried out under very harsh conditions [5, 19], orthogonal and click-chemistry techniques allowed mild reaction conditions, complex design strategies and upscaling of the synthesis [20–22]. Furthermore, a variety of single-chain architectures has been introduced from single block and multiblock to star particles, hairpins and tadpole molecules, in part aimed at approaching naturally occurring materials, such as proteins [23–26].

Proteins occur in biological organisms and display a wide variety of functions including for example structural support, transport, and catalysis. Proteins in nature are directly translated from the corresponding RNA, one amino acid after another, by ribosomes resulting in perfectly defined structures (PDI = 1) with exquisite control over composition and (dynamic) function. In situ synthesis of proteins is limited by the number of amino acids, sequence length and/or maintained function of the proteins [27]. Therefore, not only synthetic proteins, but also protein-like materials are highly sought after, for example aiming at increasing biocompatibility of materials. Moreover, the substrate specificity of proteins is not surpassed by synthetic means and is therefore of great interest in catalysis applications or in cell targeting. To achieve such functions, cooperative binding effects are pivotal, which may be provided by synthetic polymer analogues.

A wide range of design strategies for SCNPs has been developed to adjust the properties of polymers and particles. Next to broadening the synthetic toolbox and achieving control over size and SCNP folding, recent work has focused on designing SCNPs towards (biomedical) applications. In particular their small size can be expected to cause unusual biodistribution behavior [28]. For nanoparticles below 6 nm, full renal clearance is to be expected, which would certainly increase biocompatibility, but also limit their potential to short-time applications [29]. When regarding distribution studies of nanomaterials in general, size plays a major role. Whereas liposomes of < 200 nm have been reported to accumulate in the spleen, liposomes below 70 nm are

* Corresponding author at: Department of Biomolecular Nanotechnology, MESA+ Institute for Nanotechnology and TechMed Institute for Health and Biomedical Technologies, Faculty of Science and Technology, University of Twente, P.O. Box 217, 7500 AE Enschede, The Netherlands.
E-mail address: j.m.j.paulusse@utwente.nl (J.M.J. Paulusse).

https://doi.org/10.1016/j.jconrel.2018.07.041
Received 13 June 2018; Received in revised form 17 July 2018; Accepted 27 July 2018

predominantly found in the liver after IV administration to mice [30]. For gold nanoparticles, series of differently sized nanoparticles (10–250 nm [31] and 15–200 nm [32]) were intravenously administered to mice and rats respectively and only the smallest species (10 nm and 15 nm respectively) were detected in the rodents' brains [31, 32]. Further, 15–100-nm-sized gold nanoparticles were also evaluated in terms of tumor uptake and penetration depth *in vitro* and *in vivo*, and accompanied by simulations, showing increased tumor penetration depths for smaller nanoparticles with increased tumor tissue size [33]. In general, size plays a central role in the biodistribution and lifetime in the body of nanomaterials [28]. The exact size of polyamidoamine dendrimers has for example been demonstrated to play a crucial role in their cell uptake and blood-circulation times [34]. Whereas dendrimers of 6.7 nm accumulated in the brains of dogs, dendrimers of 4.3 nm were undetectable. Consequently, proper size determination and tuning is crucial for *in vivo* analysis.

The intramolecular interactions in SCNPs, which establish their 3D-structure, and the exceptionally small sizes of SCNPs, may give unique advantages in these biomedical applications, in particular in targeting elusive or difficult to reach tissues, such as the brain or dense tumors, while harnessing a therapeutic cargo. This review focuses on the design parameters for SCNPs to ready them for biomedical applications, such as protein mimicry, controlled drug delivery, and targeted imaging applications.

2. Characterization of SCNPs

The unusually small size of SCNPs may complicate their characterization. However, a combination of characterization techniques ranging from size exclusion chromatography (SEC), to light scattering and NMR techniques, have been successfully used to determine SCNP sizes, their size reduction and the particles' morphologies.

The relative size reduction from polymer to collapsed SCNP is typically observed by SEC as an apparent size reduction due to the reduced hydrodynamic radius of SCNPs [35]. Additionally, SEC coupled detectors such as refractive index (RI), UV-vis, multi-angle light scattering (MALS)/static light scattering (SLS), fluorescence and viscometers can provide further information about the SCNPs. Self-assembled SCNP structures can be even more challenging to analyze via chromatography methods, as supramolecular interactions are concentration and solvent dependent and comparable reference polymers are not always available. Berda and co-workers demonstrated the usefulness of a SEC coupled MALS detector, which was sensitive to multi-chain aggregates, which were not detectable with an RI detector [11, 36]. MALS analysis further confirms a preserved (absolute) molecular weight of polymer and SCNP, despite differing elution times/hydrodynamic radii. The SCNP radius of gyration (R_g) cannot be determined by MALS as SCNPs are usually smaller than 10 nm. Instead, intrinsic viscosity ([η]) obtained by a SEC coupled viscometer reveals R_H, which should be in line with the elution order from the column. Additionally, viscometric data yield the Mark–Houwink–Sakurada parameter *a*, which is related to the excluded volume parameter or scaling exponent (ν) from the Flory mean field theory of a self-avoiding polymer chain [37]. Both parameters provide information on the coiling degree of the polymer or SCNP and can also be estimated in the bulk [37–39].

Commonly, sizes of polymers and nanoparticles in solution are obtained from dynamic light scattering (DLS) based on their diffusion in solution, which influences the fluctuation in scattering intensity. Intensity of the scattered light is dependent on particle radius to the 6th power, and hence more sensitive for larger particles. To circumvent this influence of bigger structures on scattering intensity, DLS in material science is often transported to number or even volume plots under the assumption of the Mie theory, which makes the distribution more error-prone and larger particles are neglected [40, 41]. As these assumptions are not necessarily fulfilled for SCNPs, one must make careful use of such plots and only as complementary information. Similar to DLS, diffusion ordered spectroscopy (DOSY) NMR determines sizes based on the diffusion of particles, and hence, can be used by to verify DLS data without the influence of scattering [16, 42]. Additionally, viscometric measurements provide also the hydrodynamic radius (R_H), as well as [η], which drops in case of merely intramolecular cross-linking.

In contrast to MALS, small-angle neutron scattering (SANS) and small-angle X-ray scattering (SAXS) measurements can provide R_g also for structures < 10 nm. Additionally, ν is obtained via the form factor [38]. Fitting of theoretical form factors can attribute geometrical shapes, such as coils and spheres, to the SCNP structure and emerging minima in the intensity profile gives further information about how monodisperse and defined the SCNP structure is [43–47]. However, access to small angle facilities and instruments limits the practicality for routine experiments of this approach.

High resolution imaging techniques, such as atomic force microscopy (AFM) and transmission electron microscopy (TEM), have enabled detailed imaging of SCNPs. However, these methods image the particles in the dry state and are usually at their resolution limits for such small particles, and therefore only of limited use in determining size differences. Nonetheless, AFM was successfully applied to support SCNP size differences observed by other methods such as SEC and DLS and is even suitable for dynamic systems [13, 42, 48–51]. For this purpose, the measured height and radius of the particle can be used to deduce sizes of spherical particles, assuming globular particles in solution.

Conventionally, SCNP formation is conducted under ultra-high dilution conditions (≪1 mg/mL) to avoid multi-chain constructs. However, this technique limits the feasibility of SCNP formation in particular with regard to scalability for industrial applications. Hawker and coworkers introduced the continuous addition technique for SCNP preparation, where the polymer is slowly added to a solution suitable for cross-linking [5, 20]. In this procedure, the polymer is collapsed upon an external stimuli, such as temperature or a cross-linker molecule and the slow addition allows a low local concentration in the moment of cross-linking, enabling much higher concentrations in total (up to 10 mg/mL) [52–54]. Essential for this approach is a fast, efficient and stable cross-linking technique and it is hence, not applicable for dynamic or self-assembled systems. Alternatively, application of bulky, shielding polymer moieties, such as PEG, allowed SCNP formation at up to 100 mg/mL for both cross-linked [55, 56] and self-assembled systems [16, 57, 58]. Both approaches allow SCNPs in gram-scale, as long as the nanoparticles itself are stable.

3. Design of SCNPs as biomaterials

Selection of the polymer precursor determines the majority of the final SCNP properties and is therefore crucial in its design as biomaterial. A thermoresponsive polymer will result in a thermoresponsive SCNP [42]. Moreover, size and density of SCNPs are defined by the length of the polymer and its degree of collapsing as will be discussed in Section 3.3. Consequently, control over the properties of the precursor polymer results in control over the SCNPs. For this reason, living/controlled polymerizations, such as reversible addition − fragmentation chain-transfer (RAFT) polymerization, atom transfer radical polymerization (ATRP), ring-opening metathesis polymerization (ROMP), nitroxide-mediated polymerization (NMP) are most commonly employed in precursor polymer synthesis. Furthermore, controlled polymerization techniques provide control over composition, e.g. random vs. multiblock vs. gradient copolymers. However, biosynthetic polymers based on dextran [52] and poly(γ-glutamic acid) (γ-PGA) [43, 59, 60] have also been successfully utilized as SCNP precursors. Such well-established and approved biological precursors introduce naturally occurring motifs to the particles and increase adoption of biocompatible SCNPs. Another way of resembling naturally occurring motifs has been recently approached by equipping SCNPs with synthetic sugar moieties – either by employing carbohydrate glycomonomers for the precursor

[61] or by functionalization after SCNP formation [62].

Finally, also the SCNP formation technique influences its final properties. Stability of the SCNP structure is basically determined by the employed cross-linking technique, whether the interaction is irreversible covalent, dynamic covalent or supramolecular. Dynamic cross-links are stable under certain conditions, and *vice versa* can be cleaved under different conditions and hence introduce a trigger, such as pH [63], temperature [12], redox [64], and light [65, 66] for formation and opening of the SCNP in water, which may aid controlled drug release from the particles or provide structural changes that promote retention in tissues of interest. In a similar manner, supramolecular interactions can be tuned, as seen in examples of β-cyclodextrins (β-CD), which can be thermoresponsive [67] or redox-responsive [68]. Even permanent cross-linkers can introduce further properties to the particles, such as pH-responsiveness, metal complexation or fluorescence [8, 11, 69].

3.1. Towards water

The first requirement to developing SCNPs into a biomaterial is to render them water-soluble or water-dispersible. In principal, four general strategies can be distinguished in achieving water-soluble SCNPs: 1.) preparation of SCNPs in organic media and post-formation functionalization of these particles; 2.) direct cross-linking of water-soluble polymers in water or from amphiphilic random copolymers – 3.) either to equip SCNP with amphiphilic properties or 4.) to induce unimolecular self-folding in water. These design strategies are discussed below (Fig. 1).

3.1.1. Post-formation modification of SCNPs

Covalently cross-linked water-soluble systems based on water-insoluble precursors have been successfully obtained by post-formation modification (Table 1). In one of the earliest examples of water-soluble SCNPs, a benzothiophene derivative, 5-vinyl-1,3-dihydrobenzo[c]thiophene 2,2-dioxide, was utilized as cross-linkable unit and copolymerized with benzyl acrylate via nitroxide-mediated polymerization in DMF [19]. The cross-linking to form SCNPs occurred at 250 °C and subsequent to the formation, benzyl units were cleaved off with H_2 over Pd/C to yield carboxylic acid-functionalized SCNPs. In a follow-up study, the carboxylic acid moieties were further modified with amines for conjugation of fluorophores, dendritic structures and peptides, achieving the first SCNPs for biomedical purposes as validated in cellular uptake experiments [70]. Likewise, benzyl acrylate SCNPs, prepared via Bergman cyclization, were rendered water-soluble [71]. After cleaving the benzyl moiety, the water-soluble SCNPs served as a size-tuning template for ZnS and CdS quantum dot (QD) formation.

In a similar manner, *t*-butyl protected copolymers were applied to prepare carboxylate SCNPs [8]. In acetone, *t*-butyl methacrylate was polymerized with 2-chloroethyl methacrylate, which was later converted into an azide for Cu(I)-catalyzed click cross-linking. The employed diazide cross-linker enabled Gd(III) complexation for potential use as contrast agent in magnetic resonance imaging (MRI). After SCNP formation, the *t*-butyl group was removed by trifluoroacetic acid (TFA) to render them water-soluble. A similar deprotection strategy was used for cross-linking of an ABA block copolymer with a semiconducting B block and *t*-butyl acrylate/cross-linking unit A block [72]. The protecting group was cleaved of before nanoparticle formation; however, the carboxylic acid groups were not sufficient to obtain water solubility. After SCNP formation via benzocyclobutene cross-linking, the carboxylic acid groups were functionalized with polyethylene glycol (PEG) amines to render them water-soluble.

Two approaches to render SCNPs water-soluble were demonstrated on polymers of norbornene dicarboximides derivates by ROMP to yield unsaturated moieties [73]. Polyolefins were cross-linked via ring-closing metathesis (RCM), producing even more unsaturated bonds. Water solubility of the SCNPs was achieved by hydroxylation of the alkene bonds in the backbone with osmium tetroxide and *N*-methylmorpholine *N*-oxide, as well as by copolymerizing solketal functionalized norbornene dicarboximides and cleaving the acetal groups under acidic conditions after SCNP formation. These RCM SCNPs were used as a platform for systematical investigation of the effect of surface modification on cellular uptake as discussed in Section 3.4 [74]. To overcome the harsh reaction conditions (i.e. K_2OsO_4), Zimmerman and coworkers optimized their protocol by increasing the amount of solketal groups in the particle via using a polysolketal dendritic monomer, replacing potassium osmate completely with TFA [75]. The optimized protocol was compatible with an array of fluorescent co-monomers.

Recently, solketal methacrylate was employed to achieve water-soluble SCNPs via two strategies. RAFT polymerization of a xanthate methacrylate with solketal methacrylate yielded a copolymer with protected thiol and glycol moieties [76]. Whereas the thiol moieties are liberated by amines, the acetal group was cleaved off at low pH. Besides cross-linking the deprotected glycol polymer directly in aqueous environment, the reversed order, i.e. preparing SCNPs in dichloromethane and subsequently deprotecting the acetal groups for water solubility, was demonstrated as well. Both strategies were demonstrated to be effective in drug encapsulation. Consequently, formation of comparable SCNP can be carried out both in apolar and polar solvents, which decreases the effects of drug lipophilicity on the encapsulation process.

3.1.2. SCNP formation in water

As summarized in Table 2, several strategies for covalently cross-

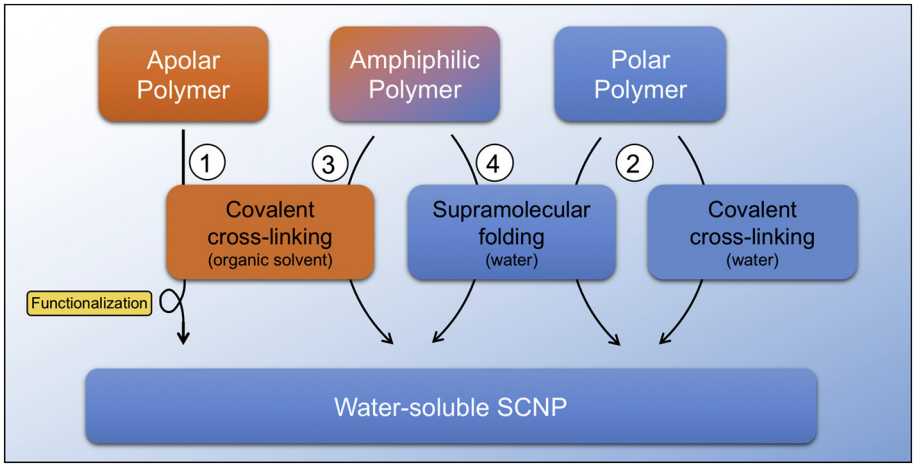

Fig. 1. Schematic overview of employed strategies to prepare water-soluble SCNPs.

Table 1
Overview of post-formation functionalization methods to render SCNPs water-soluble.

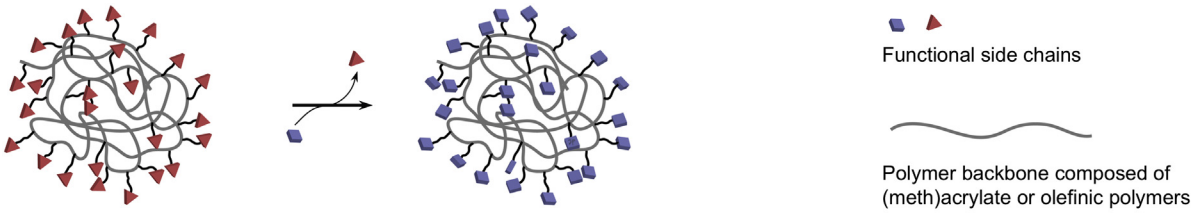

Before functionalization	After functionalization	Method	References
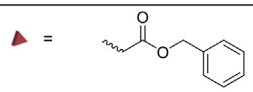		H_2, Pd/C	[19, 70, 71]
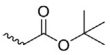		TFA	[8, 72]
	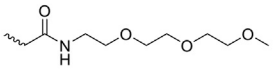	activated chloroformate reaction	[72]
		K_2OsO_4	[73, 74]
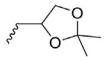		TFA / H^+	[73-76]

linking SCNPs directly in water have been developed, for example based on amidation of carbonyl groups [12, 59]. All water-tolerant intramolecular cross-linking techniques have in common their mild reaction conditions. As such, carboxyl groups of biosynthetic γ-PGA were cross-linked at basic pH with (ethylenedioxy)diethylamine activated by a carbodiimide, aiming for novel drug carriers [59].

Dynamic cross-linkers, in the form of acyl hydrazones, were introduced into a PEG-MA copolymer with aromatic aldehydes to prepare responsive SCNPs (Fig. 2) [12]. At pH 4.5, SCNPs displayed gel formation upon heating above the lower critical solution temperatures (LCSTs, 40–60 °C) and, importantly, the process was reversible upon cooling. SCNPs were reobtained after days to months, as confirmed by SEC and DLS measurements. At pH 7, however, the hydrazine linkages were stable and, hence, SCNPs and gels, formed at pH 4.5, did not interconvert upon temperature changes. Also, for irreversible cross-linked SCNPs, no hydrogel formation with increasing the temperature above the LCST was observed. Double stimuli-responsiveness makes such systems interesting for drug release materials with hydrogels serving as a constantly releasing nanoparticle reservoir.

A similar aldehyde amidation technique was further utilized by Fulton and co-workers to functionalize benzaldehyde moieties of polyacrylamide polymers with either mannose or galactose benzoyl hydrazides [62].Via transamination with succinic dihydrazide, intramolecular cross-link were introduced. SCNPs with specific molecular recognition by surfaces coated with Concanavalin A or with *Escheria coli* (*E. coli*) heat labile toxin, respectively, were successfully developed. The carbohydrate functionalized SCNPs formed a film on the complementary surfaces, whereas on the mismatched surfaces no film formation was observed by AFM. Likewise, dynamic cross-linking was crucial in formation, highlighting the importance of interchain cross-links in film formation.

Functional SCNPs were prepared from poly(methacrylic acid) conjugated with alkoxyamine groups, which were reacted with aldehyde groups of a diethylenetriaminepentaacetic acid (DTPA) derivate at pH 6 [77]. DTPA further served to chelate ^{67}Ga for single-photon emission computed tomography (SPECT) imaging *in vivo*, and activated carboxylic acids were utilized for amide formation with a peptide targeting agent against pancreatic cancer.

In a completely different fashion, amphiphilic mono-tethered SCNPs, based on a poly(ε-caprolactone)-s-s-poly(2-(dimethylamino) ethyl methacrylate (PCL-S-S-PDMAEMA) block copolymer, were applied to act as surfactant for suspension polymerization of styrene in water [78]. In this procedure, 1,4-diiodobutane intramolecularly quaternizes the tertiary amine of the PDMAEMA block and hence, producing a cationic head, which aligns to the aqueous phase in suspensions.

Recently, Barner-Kowollik and co-workers transferred their previously developed SCNP formation by nitrile imine-mediated tetrazole–ene cycloaddition (NITEC) to water [69, 79]. Via light-induced cross-linking between tetrazole (Tet) and maleimide (Mal) derivates under high dilution (0.017 mg/mL), fluorescence arises upon SCNP formation due to the pyrazoline adduct. Applying poly(acrylic acid) (PAA) as the backbone for water-soluble precursors, led to a competing reaction between the tetrazole and the carboxylic acid moieties, referred to as nitrile imine-carboxylic acid ligation (NICAL). In contrast to reactions between polymers and small molecules, NITEC was preferred over NICAL as intramolecular cross-linking reaction, resulting in a fluorescence emission max. of ~560 nm. On the other hand, SCNPs prepared from PAA with conventional triazole functionalization, and therefore formed exclusively by NICAL cross-linking, displayed blue shifted fluorescence properties with an emission max. of ~520 nm. Further, the Tet and Mal functionalities were conjugated on a mannose methacrylate polymer to form glycopolymeric SCNP [61]. For this purpose, acetyl-protected mannose methacrylate was RAFT polymerized, and after deprotecting Tet and Mal acids were conjugated to the polymer via EDC coupling to enable SCNP formation. Inspired by viruses, the obtained carbohydrate SCNPs were coated on nanodiamonds to promote cellular uptake of the nanodiamonds.

As thiol-Michael addition can take place in organic media as well as in (basic) water, it has also been employed as intramolecular cross-linking technique in water - using both acrylate- and thiol-containing

Table 2
Intramolecular cross-linking methods for SCNP formation in water.

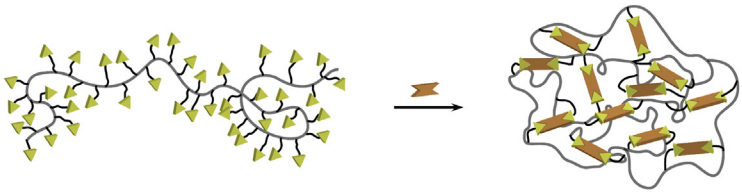

Polymer backbone composed of dextran, (meth)acrylate or γ-glutamic acid polymers

Type of reaction	Cross-linking moiety on polymer	Complementary cross-linking moiety	References
amidation		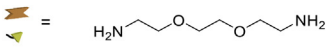	[59]
	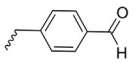	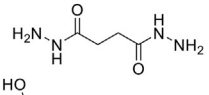	[12, 62]
	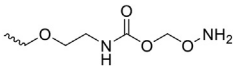	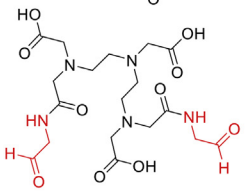	[77]
quaternization	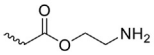	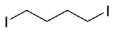	[78]
NITEC	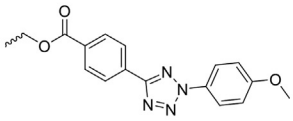	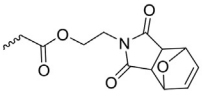	[61, 69]
NICAL			[69]
thiol-Michael addition		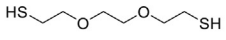	[52, 80]
	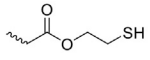	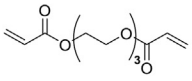	[76]
Host-Guest • Cucurbit[x]uril	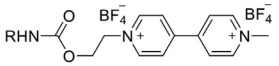	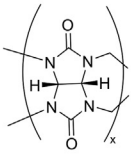 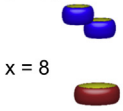	[50]
	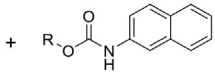		[81]
• β-cyclodextrin	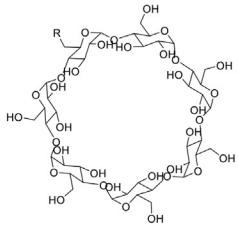	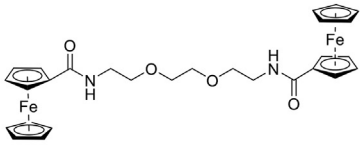	[68]

polymer precursors [52, 76, 80]. For the first, the biopolymer dextran was decorated with methacrylates and cross-linked via a dithiol. Alternatively, thiol-protected monomers were copolymerized with water-compatible monomers via RAFT polymerization and after deprotection, reacted with a diacrylate cross-linker. In both cases, mono reactive species were utilized for post-formation functionalization – either for fluorescence labeling or for radiolabeling as applied in initial *in vivo* studies [52, 76]. Likewise, an antigen mimetic was added to the dextran SCNPs in order to trigger immune response [80].

Proteins fold in water mainly due to supramolecular interactions in water. Supramolecular assembly of polymers, using host-guest interactions with *nor-seco*-cucurbit[10]uril (CB[10]) or with cucurbit[8]uril

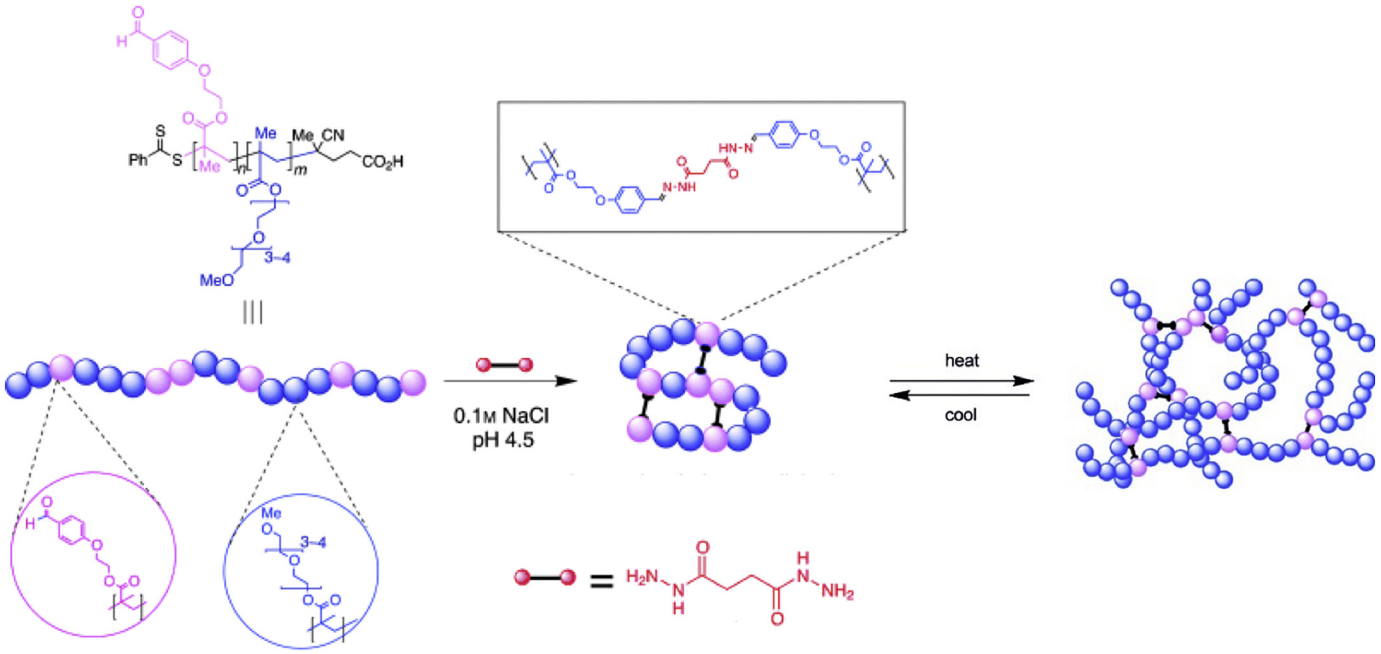

Fig. 2. Formation of dynamic covalently cross-linked single-chain polymer nanoparticles in water, and reversible gel formation upon heating. Adapted from ref. [12] with permission of John Wiley Sons, Inc. (2012).

(CB[8]) as cross-linking method, is readily performed in water [50, 81]. Poly(*N*-hydroxyethylacrylamide) (pHEAA) was prepared by ATRP and functionalized with methyl viologen as a guest. By addition of CB to the aqueous polymer solution (with ≤0.1 mg/mL), nanoparticles between 30 and 50 nm in hydrodynamic radius were obtained. Higher concentrations of the polymer resulted in multi-chain assemblies. Further, β-CD as an established host, conjugated onto acrylamides, resulted in SCNP folding in water. In this procedure, pHEAA, partially reacted with tosyl β-CD, self-assembled upon addition of bridged bis(ferrocene) in ethanol solution to yield redox-responsive SCNPs [68]. In a different class of supramolecular SCNPs, metal-coordination in water is exploited (Table 3). 2-Hydroxypropylmethacrylamide (HPMAA), as either block or random copolymer with an imidazole acrylamide, were prepared via aqueous RAFT polymerization and have shown to form SCNP complexes with copper(II) at low pH [82, 83]. The lower the pH, the more imidazolium units were ionized, which caused weaker Cu(II) coordination and simultaneously, increased electrostatic repulsion between the particles. Above pH 5.5, the block copolymer SCNPs started to assemble into larger structures, such as micelles, and larger networks, whereas the SCNPs from random copolymers with 9% imidazole monomer units formed stabled nanoclusters of 18 nm, which proved to be redox-responsive. Furthermore, Cai and co-workers demonstrated a dual folding of an ABC HPMAA block copolymer with an imidazolium and a quaternary amine moiety block, resulting in two individual Cu(II) coordinating compartments [84]. A less pH sensitive approach towards SCNP folding via copper complexation was demonstrated by Bai *et al.* [85]. Cu^{2+} was chelated by aspartate, whereas imidazolium alkyl groups permit hydrophilic particles with hydrophobic compartments. Reduction to Cu(I) was performed to furnish the particles with catalytic activity in cellular environment with reasonable cell viabilities. Besides copper, Fe^{2+} ions were also successfully applied to induce SCNPs collapse [86]. Addition of pHEAA containing 5 or 10% terpyridine functionalized ethyl acrylate to a 60 °C heated $FeCl_2$ solution led to SCNP formation as was accompanied by a color change. Metal-coordinating SCNPs resemble metal-coordinating proteins and may therefore have useful applications as biomaterials for catalysis. Despite metal associated toxicity, primary cell toxicity studies did not reveal cytotoxic effects of the tested materials as will be discussed below.

3.1.3. SCNPs from amphiphilic random copolymers

In addition to polymer cross-linking in water, amphiphilic random copolymers (ARPs) are *i.a.* utilized to covalently cross-link polymers intramolecularly in organic solvents and endowing them with amphiphilic solubility. For example, Cu(I) catalyzed click chemistry was performed in DMF on a NIPAM copolymer with alkyne and azide functionalities, resulting in water-soluble SCNPs [42]. pNIPAM further supported intramolecular photodimerization of coumarin-moieties in THF [66]. THF is a good solvent for coumarin, hence preventing formation of multi-chain aggregates, but also slows down cross-linking. Contraction of SCNPs was observed upon dialysis to water, which was assigned to the hydrophobicity of coumarin. PEG methyl ether methacrylate (PEG MA) even granted water solubility when employed as a comonomer to polystyrene SCNPs with benzimidazolium cross-links [87]. Poly(PEG acrylate)-(ε-caprolactone acrylate) copolymers were further intramolecular cross-linked by ring-opening polymerization in chloroform and achieving water-soluble SCNPs, which were further tested on cells with a view to application as drug delivery agent [55]. In addition, 4-acryloylmorpholine and hydroxyethyl acrylate (HEA) copolymer was employed to allow isocyanate cross-linking in dichloromethane and still prepare water-soluble SCNPs [88].

After Berda and co-workers employed redox-responsive disulfide containing cross-linkers for SCNPs in THF [11], the group of Thayumanavan developed water-soluble SCNP that were formed through formation of disulfide bridges [64, 89]. In the presence of dithiothreitol (DTT), pyridyldisulfide units in a hydroxyethyl methacrylate (HEMA) copolymer underwent disulfide exchange in methanol to form SCNPs as will be discussed in Section 4.2. The concentration of DTT determined the extent of disulfide-thiol exchange and the size of the formed SCNPs. In contrast, SCNP formation was found to be reversible at high levels of DTT. According to the authors, the selection of a good (organic) solvent is important to avoid multi-chain aggregation and to allow SCNP synthesis at concentrations of up to 10 mg/mL. Nevertheless, the incorporation of HEMA moieties was sufficient to render the disulfide SCNPs water-soluble.

Furthermore, ARPs can undergo solvent-driven self-sorting into unimolecular particles without site-specific interactions (ARP-SCNPs). These self-sorting interactions can be classified into two types: self-folded SCNPs (for predominantly hydrophilic ARPs) [90–93] and

Table 3
Self-complementary supramolecular interactions for SCNP assembly in water.

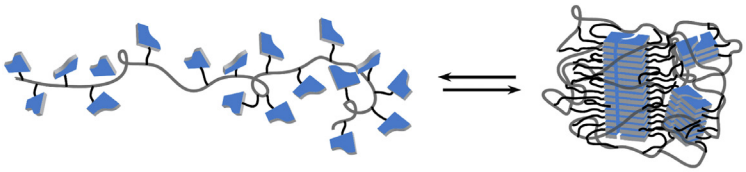

Polymer backbone composed of (meth)acrylate polymers

Type of interaction	Supramolecular moiety		References
Metal-coordination • Cu(II)	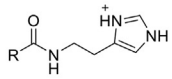		[82, 83]
		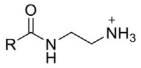	[84]
	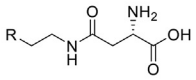		[85]
	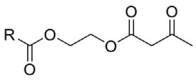		[100, 101]
• Fe(II)	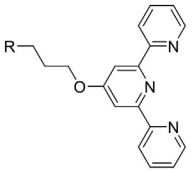		[86]
Hydrogen-bonding • urea	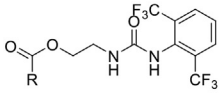		[44]
• urethane	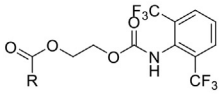		[44]
• U-DPy	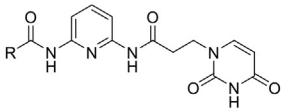		[102, 103]
BTA	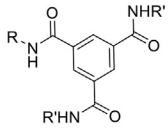	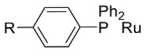	[45, 104, 108, 109] [16, 105, 106]

collapsed, so-called colloidal unimolecar polymers (CUPs) (for predominantly hydrophobic ARPs) [94–96].

3.1.3.1. Self –folding amphiphilic random copolymers. Whereas amphiphilic diblock copolymers usually undergo formation of multi-chain structures for phase separation, ARPs can self-fold into unimolecular solubilized micelles, and are likewise also considered SCNPs [91]. If in an appropriate ratio, the hydrophobic/hydrophilic interactions of the amphiphilic monomers drive the copolymer to intramolecular self-assembly. To yield amphiphilic, water-soluble random copolymers, either hydrophilic/ionic or amphiphilic monomers, such as NIPAM or PEG MA, as extensively studied by Sawamoto and co-workers, are polymerized with lipo- or fluorophilic monomers [90–93]. For water-compatible SCNPs, the polymerization is usually conducted in organic environment, whereupon the self-folding takes place in aqueous environment. Whereas ionic ARPs may display pH-responsiveness, PEG and NIPAM monomers introduce thermo-responsiveness [97]. Alternatively, the group of Akashi grafted γ-PGA with phenylalanine, resulting in polymers of 140 kg/mol, which form SCNPs in water [43, 60]. Another ARP grafting approach was shown by Baglioni and co-workers with grafting PEG with poly(vinyl acetate) (pVAc), which has been utilized for encapsulation of small molecules as will be discussed later [98].

Considering that these ARP SCNPs consist primarily of the employed

copolymers without additional steps, it is the most straightforward SCNP synthesis - especially since even free radical polymerized copolymers have yielded unimer aggregates [57, 93]. However, concentrating these unimolecular micelles has limitations, as larger aggregates will form, even though PEG ARPs were stable at 100 mg/mL for over 4 months [57]; and the stability of these SCNPs depends strongly on environment and temperature. Combination of self-folded copolymers with cross-linking techniques fixates the folding of the polymer or pre-folds the polymer for cross-linking. In this respect, PEG MA increased the stability of micelles when equipped with a dodecyl methacrylate core and enabled radical cross-linking of methacrylate-decorated HEMA at rather high concentration (10 wt%) [25]. In a similar matter, aromatic groups in a poly(*N*-phenyl)/acrylamide/acrylic acid ARP supported the amidation with hexamethylenediamine of carboxylic acids in acetonitrile and higher incorporation ratios of phenyl groups resulted in denser SCNPs [99].

Pomposo and co-workers studied copper-induced SCNP folding with an amphiphilic random PEG MA copolymer in both THF and water [100, 101]. 2-Acetoacetoxy ethyl methacrylate (AAEMA) was utilized to chelate copper and provided the polymer with hydrophobic units. Further, they demonstrated through SAXS measurements and molecular dynamics simulations, that cross-linking in water as a bad solvent for AAEMA, led to more globular SCNPs than formation in THF.

Furthermore, self-sorting has been applied successfully to support hydrogen-bonding motifs in SCNP formation in water. Sawamoto and co-workers demonstrated the self-assembly of hydrophobic urea- and urethane-functional motifs in random PEG MA copolymers into SCNPs [44]. Similarly, self-complementary sextuple hydrogen-bonded uracil-diamido-pyridine (U-DPy) motifs form dimers in such PEG MA copolymers [102, 103]. Random incorporation of methacrylate functional chiral benzene-1,3,5-tricarboxamide (BTA) moieties even resulted in the formation of helical aggregates with hydrophobic cavities and demonstrated catalytic activity in water upon incorporation of a ruthenium complex [16]. In order to prepare water-soluble BTA ARPs with controlled composition by post-polymerization functionalization, the PEG was replaced with polyetheramines (Jeffamine) [104]. These BTA ARP SCNPs were further utilized in several enzyme-mimicking catalysis studies in water [104–109].

3.1.3.2. Colloidal unimolecular polymers (CUPs). Colloidal unimolecular polymers (CUPs) are unimolecular aggregates of polymers collapsed due to the hydrophilic/hydrophobic interactions between polymer and solvent [94–96]. Contrary to self-folding amphiphilic random copolymers (vide supra), CUPs are ARPs that are insoluble in water and situated as a suspension in water. Formation via stripping of organic solvent from a water/organic solvent polymer solution leads to a collapse of the hydrophobic core. Whereas the self-folding of ARPs leads to sparse structures, the collapse of hydrophobic copolymers results in compact particles with a water-free core. In this process, a hydrophobic to hydrophilic balance of around 9:1, as well as slow addition of water to the organic phase are crucial. Usually methacrylates are employed as a hydrophobic backbone, while a cationic comonomer serves as the hydrophilic counterpart, resulting in a hydration shell and stabilization of the particles by electrostatic repulsions [110, 111]. However, CUPs have not yet been consider for medical applications and will not be further considered here.

3.2. Post-polymerization/-formation modification

An extensive toolbox for post-polymerization functionalization has been developed over the years and has been applied to SCNPs as well [112]. Post-polymerization is often used to render SCNPs water-soluble or to add functionality and complexity either to the polymer or to the SCNPs, to circumvent interference with the polymerization or SCNP formation technique. A popular approach for SCNP functionalization is amidation of carboxylic acids with functional amines, such as in the addition of gadolinium(III)-chelating groups [72]. For protein conjugation to SCNPs, *N*-hydroxysuccinimide ester (NHS) and pyridyl disulfide end groups were utilized to respectively attach amine or thiol groups on the protein to fluorous ARPs for potential protein targeting [113].

Also, pentafluorophenol-ester (PFP) polymers offer an excellent platform for modifications with amines or alcohols and have been utilized to ease the SCNP precursor preparation [104, 114]. Although the pentafluorophenol-ester is very suitable for post-modification, until now it was only utilized to prepare precursors for SCNPs, but not yet to functionalize SCNPs or to render them water-soluble.

Fluorescent nanoparticles greatly facilitate their tracking in *in vitro* and *in vivo* models. Besides a selection of SCNPs systems where fluorescence arises from the cross-linking procedure, the polymer or the nanoparticle itself can be decorated with fluorescent labels as reviewed in detail elsewhere [115]. Many different fluorophores, covering a broad range of emission wavelengths (300–700 nm), have been employed in SCNP formation. Alternatively, radiolabeling of SCNPs has been successfully carried out with chelators, such as DTPA and 1,4,7-triazacyclononane-1,4-diacetic acid (NODA), binding gallium-67 (^{67}Ga), and were used in *in vivo* imaging of SCNPs [52, 77]. However, as the different SCNP systems are based on different chemistries that generally require a high degree of orthogonality, labeling still requires individual adjustment of each SCNP system.

Another important application of post-formation functionalization of SCNPs is in the incorporation of targeting moieties. For example, the addition of a pancreatic cancer targeting peptide onto carboxylic acid SCNPs via lysine moieties resulted in increased targeting in mice with induced pancreatic cancer as discussed in Section 4.2 [77]. Similarly, as pancreatic cancer vaccines, a mimic of the carbohydrate α-Tn antigen was added via a fluorinated amine spacer to carboxylic acid modified dextran SCNPs [80].

A pioneering example of SCNP post-functionalization to tune it for biomedical purposes is given by Harth and co-workers [70]. First, benzyl acrylate SCNPs were deprotected to yield water-soluble, carboxylate-functional SCNPs, which were further conjugated with ethylenediamines and maleimide PEG hydrazides. The maleimide was reacted with a mono-thiol dendrimeric unit for targeting; whereas NHS coupling was utilized for fluorescent labeling and addition of PEG groups. Finally, thiol-disulfide exchange was used to functionalize these SCNPs with fluorescently labeled peptides to study intracellular peptide delivery.

3.3. Size and density of SCNPs

Whereas size is an important factor for the nanoparticle distribution, the degree of compactness and the shape of the nanoparticles play a role when it comes to function of the nanoparticles for application such as drug delivery. The transition from a flexible chain to a compact particle is crucial for cargo encapsulation. Further, creating of cavities and compartments gives the opportunity for catalytic environments and also for space cargos. The following section will discuss how to tune SCNP in term of size, morphology, and density.

The properties of SCNPs directly originate from their polymer precursors and the employed cross-linkers. In general, larger polymer precursors lead to larger, relative size reduction and to larger particles [5, 20, 49, 116]. For UPy-based supramolecularly folded SCNPs, precursor length did not influence the relative size reduction, but resulted in bigger SCNPs with longer polymer precursors as visualized by AFM [116]. Further, it is predicted that stiffer precursor chain collapse without an explicit cross-linker leads to more globular structures as short loops are more restricted by the bending energy of the polymer [117].

Besides polymer precursor length and stiffness, also the techniques of chain collapse determine the final size of the particles. For cross-linked SCNPs, the amount of cross-links determines the degree of

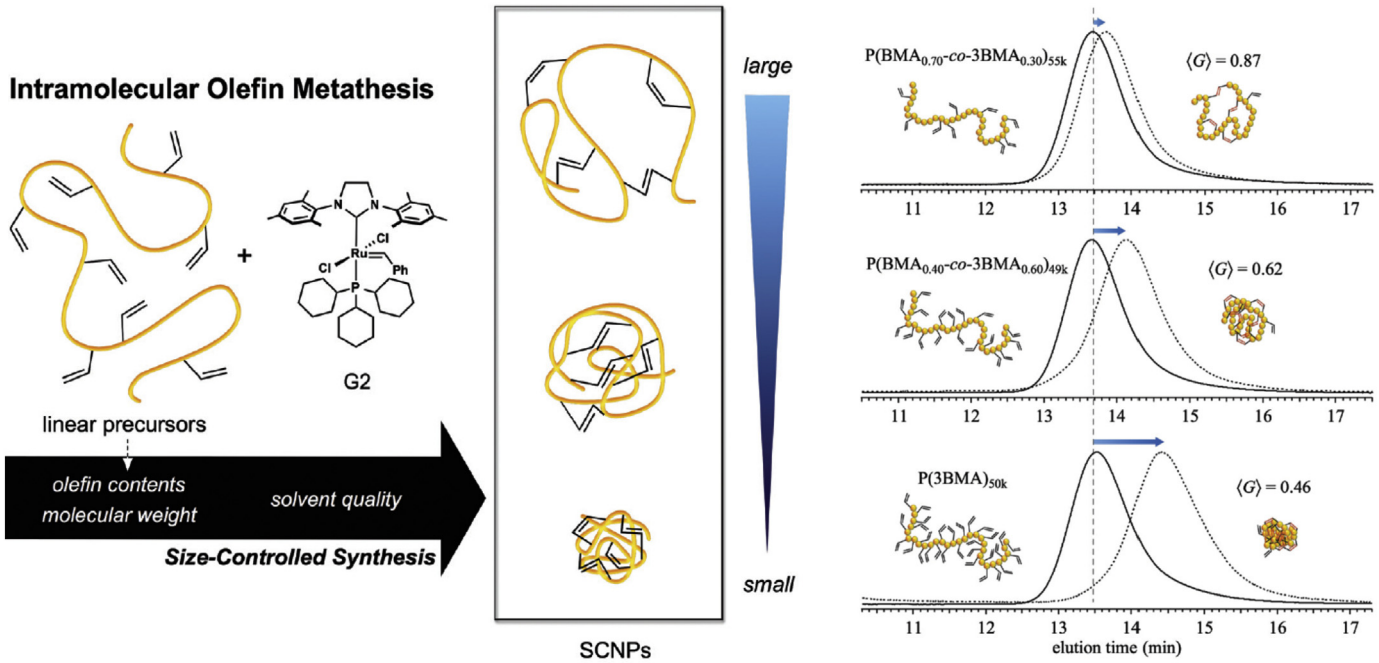

Fig. 3. Schematic representation and SEC traces of polymers and corresponding SCNPs prepared by olefin metathesis. Increased number of cross-linkable units on the polymer results in smaller and compacter particles. Reproduced with permission from ref. [118] with permission of The Royal Society of Chemistry (2016).

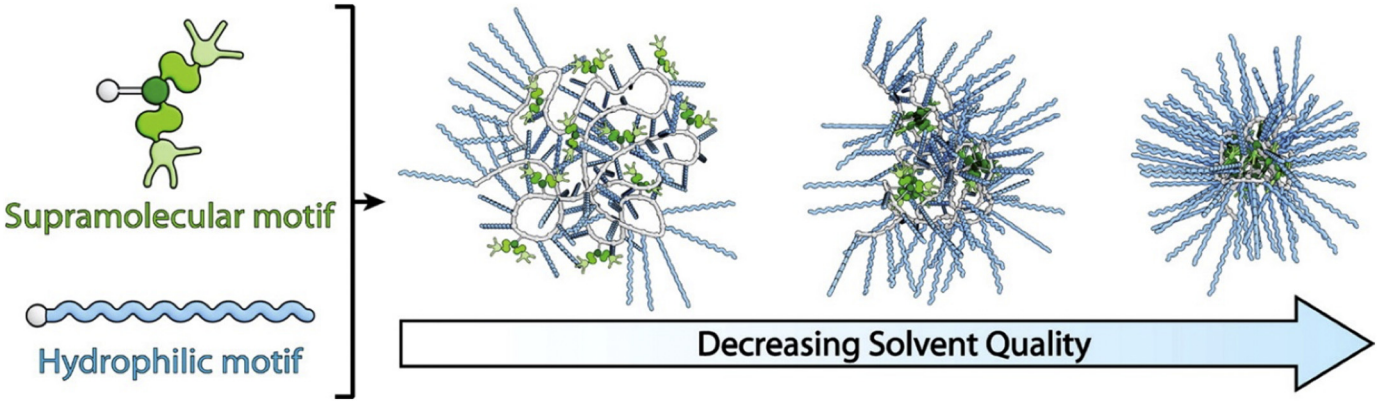

Fig. 4. Schematic representation of solvent dependency on size and compactness of bipyridine-substituted benzene-1,3,5-tricarboxamides SCNPs. Reproduced with permission from ref. [45] with permission of American Chemical Society (2015).

folding, as well as the density of particles [118] (Fig. 3). Higher degrees of cross-linking usually yield smaller SCNPs [20, 49]. AFM analysis of SCNPs prepared by olefin metathesis revealed that with increasing degree of cross-linking, the volume of the particles remained constant, but the extension on the surfaced was reduced, indicating more globular structures less prone to deformation [10]. Further increase of the compactness of SCNPs was demonstrated by combining two orthogonal cross-linking techniques [119, 120]. Not only the degree of cross-linking determines the density of cross-linked SCNPs, but also the nature of the cross-links - especially for cross-linker-mediated chain collapse. Longer cross-linkers are predicted to fold the polymer precursor more efficiently, as short cross-linkers are assumed to cause too short range loops for efficient compaction [121]. For dynamic cross-linking, however, increasing the compactness by the number of cross-links is limited by multi-chain aggregation [59]. Reversible assembly of SCNPs into superstructures may bring advantages for example as injectable macrogels that break down to smaller, structures and deliver drug-loaded particles to the site, and may thus prevent premature excretion from the body.

Similar to cross-linking density in cross-linked particles, the composition between hydrophilic and hydrophobic groups determines the compactness of ARPs [44, 91]. For supramolecular-assembled polymers, too many supramolecular motifs lead to multi-chain aggregates [122]. Furthermore, longer polymer chains can lead to elongated, less spherical structures as observed with the ellipsoidal particle form factor in SANS measurements [47]. The solubility, aggregation number, size and compactness for self-folded ARPs are tuned by composition ratio and length/molecular weight of the polymer, as well as by the length of side-chain and choice of comonomer [57, 123]. Longer copolymers lead to more compactness and likewise, more hydrophobic groups end up in denser SCNPs. The group of Sawamoto employed SEC coupled MALS supported by DLS and SAXS experiments to show that with an increasing degree of polymerization (DP) of PEG ARPs, the aggregation number decreases down to 1 and with increasing hydrophobicity, higher DPs are required. In another example with γ-PGA ARPs, an increased amount of grafting with phenyl groups increased density of the particles as shown by comparing DLS and SLS data [60]. In this case, the aggregation number was influenced by the salt concentration, as salt reduces the electrostatic repulsions and more chains aggregate together.

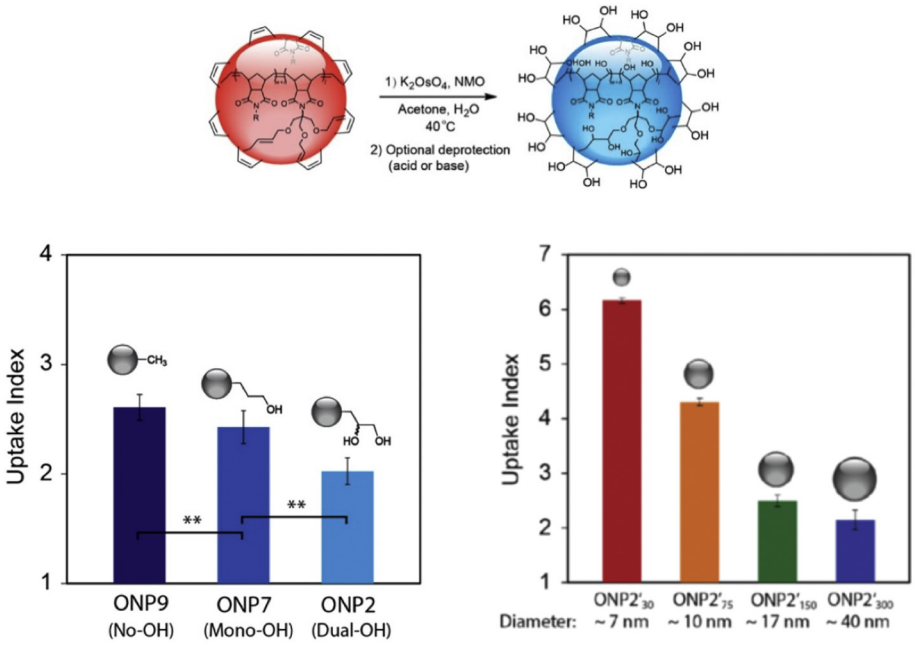

Fig. 5. Cellular uptake comparison of polyolefin SCNPs by a) surface-modification with alcohol groups; and b) on nanoparticle size. Reproduced with permission from ref. [74] with permission of American Chemical Society (2015).

The polarity of the solvent is crucial to form self-assembled SCNPs, and the resulting structure and compactness stays solvent-depending (Fig. 4) [15, 124, 125]. Whereas differential solvents plays only a minor role in biological systems, the solvent during covalent cross-linking/folding process influences the steady morphology of SCNPs, as well as the encapsulation efficiency of cargos [101, 118, 126]. As extensively studied with SAXS experiments and simulations by Pomposo and co-workers, two types of morphologies can be obtained for cross-linked SCNPs: globular protein-like structures and sparse structures, which resemble intrinsically disordered proteins [101, 126]. Especially, globular structures are of interest for enzyme-mimicking behavior and efficient drug encapsulation, but ideal globular SCNPs have been rarely achieved [38]. Cross-linking under theta solvent conditions resulted in a sparse form, whereas cross-linking in a bad solvent caused a pre-coiling and hence resulted in a more globular form. Simulations led to the conclusion that the cross-linkable unit should be solvophobic to support formation of globular structures, whereas the backbone should be solvophilic to prevent aggregation.

As to the inner structure of SCNPs, π-π stacking in organic solvents of a pentafluorostyrene and a styrene block in a triblockcopolymer, was identified by 2D NMR spectroscopy and described as single chain folding mimicking a β-hairpin motif [23]. Although this folding took place in organic solvent, 2D NMR offers potential for further investigation of inner structures of water-tolerant SCNP.

SCNPs in the wide size range of 2–50 nm in diameter have been reported over the years. Careful design of the precursor polymers and the employed intramolecular cross-linking techniques enables easy adjustment of SCNPs with respect to size, density and even morphology. In order to approach larger SCNP-like systems, controlled polymerization of *e.g.* multi-vinyl monomers yield in branched and intramolecular cross-linked nanoparticles that growth with reaction time – coined as Single-Chain Cyclized/Knotted Polymer Nanoparticles [127–130].

A critical comparison between the 'true' size of SCNPs and its characterization techniques applied in literature is presented by the group of Barner-Kowollik [131]. Evidently, not all above mentioned characterization methods reveal the same size as they rely on different aspects, such as motion in solution, collapsing on surfaces, scattering and rheological behavior. In addition, the wide range of different synthesis techniques will also result in different outcomes. Nonetheless, the large variation in size is rather surprising and it is doubtful whether all of these systems are indeed true SCNPs. To distinguish between slightly modified polymers, SCNPs and multi-chain clusters, a careful choice of characterization methods is required. In view of future applications, exclusive single-chain systems are not always essential. Even more so, small multi-chain nanoparticles may also offer advantages, provided their properties can be controlled.

3.4. Cellular uptake

Size of nanomaterials has been demonstrated on multiple occasions to matter on a cellular level. For example, Williams *et al.* demonstrated that smaller sized cadmium-based quantum dots (QDs) of 2 nm pass into the nuclei and concentrate around the nucleoli of several cell-types, but with increasing size, cell penetration was hampered. Therefore, the QDs ended up in the cytoplasm or were not taken up by the cells at all [132]. The size cut-off and cellular uptake kinetics are cell-type dependent, and nanoparticle size affects cellular uptake mechanisms [133].

Extensively modified carboxylic acid particles of the group of Harth were found to show no significant uptake to 3T3 cells after 30 min of incubation [70]. However, modification of the SCNPs with a guanidinyl dendrimeric unit yielded a strong fluorescent signal distributed over the cell. Disulfide-coupled peptide as a cargo was also successfully delivered into the cell, but the signal did not fully co-localization with the nanoparticles. Likely, disulfide bonds were cleaved, but different fluorophore lifetimes impeded the measurements and the final destinations of nanoparticles and cargo could not be identified.

Codelivery of cargo and SCNPs to hCMEC/D3 cells was further shown by Paulusse and co-workers [76]. Glycol SCNP of ~10 nm were taken up by the cells within 20 h without ending in the lysosomes. When Nile red was encapsulated as a model drug, nanoparticles and Nile red co-localized within the cells.

Zimmerman and co-workers studied the cellular uptake behavior of their SCNPS prepared by ring-opening and ring-closing metathesis on HeLa cells [73, 74]. With confocal microscopy and FACS measurements, uptake of 15-nm-sized SCNPs was observed following 6 h of incubation, whereupon the SCNPs were found in the lysosomes [73]. Despite cellular uptake, no cytotoxic effects of smaller sized particles

(15 nm) and only minor effects of larger particles (50 nm) were observed when exposing HeLa cells to the SCNPs at a concentration of 10 μM (0.5–1.0 mg/mL), which might also be assigned to residual osmium and ruthenium ions in the samples as a result of the synthetic procedure, according to the authors. Subsequently, the size-dependence of uptake (7–40 nm), as well as the dependence on particle surface chemistry were systematically investigated in a follow-up study (Fig. 5) [74]. After 3 h of incubation, the smallest particles displayed 3-fold higher uptake as compared to the largest particles and a clear overall size trend was revealed. Further, monomers with different hydrophilicities were employed in the formation of ~10 nm SCNPs. Increased alkyl chain length and reduced alcohol moieties, i.e. increased hydrophobicity, promoted cell uptake of SCNPs. Addition of serum to the particles to provide a protein corona yielded comparable polarity trends, but with diminished cell uptake. Because of the lysosomal uptake in the initial studies, receptor-mediated endocytosis was postulated. Therefore, cell-uptake experiments were also conducted at 4 °C. At these decreased temperatures, hardly any uptake was detected, which further supports that receptor-mediated endocytosis takes place. With an adjusted protocol excluding osmium ions, rather using dendronized glycerol units, a series of SCNPs with different fluorophores was evaluated on HeLa cells with high cell viabilities in all observed cases (≥85% at 0.1 mg/mL) [75]. Furthermore, the fluorescent signal was detected mainly in endosomes after 4 h, as was also the case in the previous studies, but appeared also in the cytoplasm of the HeLa cells. Further investigations of the cell uptake mechanism are pending.

Zimmerman and co-workers further demonstrated an indirect way to observe cellular uptake of metal-complexing SCNPs through intracellular catalysis [85]. The SCNPs based on alkyl imidazole ROMP copolymers containing copper(II)-aspartate complexes as catalytic systems were able to catalyze a click reaction to convert a non-fluorescent compound into a fluorescent dye. SCNPs of 10 nm were administered to human non-small-cell lung carcinoma (NCL-H460) and human breast cancer (MDA-MB-231) cells and only the highest concentrations (0.03 mg/mL) affected cell viabilities, though these concentrations were considered sufficient for intracellular catalysis studies with cells. Subsequently to washing the cells that were incubated with SCNPs, the non-fluorescent precursor was added to the cells, after which strong fluorescent signals were detected in the entire cell except for in the nuclei. The Cu(II)-loaded SCNPs were also used to catalyze a click reaction to produce an antimicrobial agent inside *E. coli* cells. While mere SCNPs did not influence cell viabilities of *E. coli* bacteria, the particles in combination with the substrates for the formation of the antimicrobial, reduced *E. coli* viability. Combining this intracellular reaction concept with cell-specific targeting properties, may enable labeling or killing cells of interest, such as cancer cells or bacteria.

Intracellular reactions with SCNPs were also demonstrated by Palmans and co-workers, who exposed self-assembled BTA Jeffamine SCNPs to HeLa cells [109]. Encapsulation of a solvatochromic naphthalimide dye confirmed intact folding of the ARP-type SCNPs in the presence of serum. As the particles ended up in the lysosomes, cells were electroporated to avoid endocytic uptake and to permit nanoparticles to enter the cytosol. BTA self-assembled Jeffamine polymers incubated on HeLa cells did not show any cytotoxic effects, even at the highest evaluated concentration of 2.5 mg/mL [109]. In case of electroporation of the cells for increased cell uptake, partial cell death was observed as may be expected. However, this effect was not increased by the presence of the particles. This approach promotes nanoparticle uptake by cells, but is not applicable to complex biological systems. In order to prevent aggregation pf porphyrins for photodynamic light therapy, PEG BTA SCNPs were also equipped with a porphyrin, which can generate single oxygen upon light irradiation. In the dark, these lysosome-located particles did not affect the cells at any of the tested concentrations. Upon irradiation with blue light, cell viabilities dropped dramatically for particle concentrations above 0.1 mg/mL. Also, catalytic carbamate cleavage reactions in cellular environment were performed with BTA SCNPs with bipyridine or phenanthroline to complexate Cu(I)/Pd(II). Successful cleavage was confirmed by fluorescence from the reaction product. The complexation of the metals with SCNPs was crucial in order to obtain their catalytic activity within the cell medium. Although the SCNPs were only applied to the extracellular matrix, fluorescence was arising from within the cells as the product presumably diffused into the cells. The catalytic reaction did not reduce cell viability below 80%, though cell morphology was altered in the case of Cu(I) catalysis.

The group of Zimmerman demonstrated how cell uptake of SCNPs may be influenced by particle properties, such as size and polarity. However, so far only a limited number of studies reports the effects of SCNP structure and composition on cellular uptake. As increased stiffness has been shown to promote cell uptake [134], uptake behavior of SCNPs is likely to differ from conventional polymer uptake mechanisms, and more detailed studies into the uptake behavior are therefore desired.

3.5. Toxicity and biocompatibility

Successful translation of SCNP technology to the clinic requires critical evaluation of a nanoparticle's toxicity. As SCNPs are prepared based on different materials, their commonality is a reduced size relative to conventional polymer nanoparticles. Consequently, SCNPs present a higher surface to volume ratio and an increased curvature, which increases the contact area of these materials with fluid environments, while decreasing the adhesion energy with membranes [135]. Furthermore, the curvature of a nanoparticle can also influence its apparent pKa [136]. Finally, small nanoparticles are less prone to accumulation in the body due to renal clearance, which reduces possible long-term risks [137]. Prior to *in vivo* studies, cell viability studies are most commonly performed with methods such as the MTT tetrazolium reduction assay, which assesses metabolic activity of the cells in comparison to non-treated cells, or live/dead staining, comparing the population of live and dead cells depending on their membrane permeability [138]. Also, hemolysis assays are conducted as safety evaluation by measuring the hemoglobin content in blood plasma assigned to red blood cell lysis [139]. Over the last years, a couple of such viability studies have also been performed on SCNPs based on a variety of different materials as will be discussed in the below.

3.5.1. ARPs

For self-folded and self-assembled ARPs, cytotoxicity is expected to arise mainly from the hydrophilic monomer, which is assumed to be at the exposed outside of the particle. Several PEG ARPs have been tested for their effects on different cell lines. As seen in the previous section, BTA self-assembled Jeffamine polymers did not show cytotoxic effects when incubated with HeLa cells [109]. Also no cytotoxic effects on embryonic kidney HEK 293 cells were observed after 24 h incubation with U-DPy self-assembled PEG polymers with concentrations as high as 0.2 mg/mL [103]. Similarly, perfluorinated PEG/PEG ARPs did not reveal any effects on NIH 3T3 (mouse embryo fibroblast) cells or HUVEC (human umbilical vein endothelial cells), with tested concentrations up to 1.0 mg/mL [113].

Series of ethyl- and butylamine containing PEG ARPs with different amounts of variable hydrophobic comonomers were designed to approach the amphiphilic nature of antimicrobial peptides that are believed to disrupted cell membranes. The obtained particles were screened for their antimicrobial activity and cytotoxicity towards H4IIE liver cells [140]. Biocompatibility was described in terms of the half maximal inhibitory concentration (IC_{50}), i.e. the concentration at which cell viability decreased to 50%. The butylamine ARPs demonstrate strongly increased toxicity as compared to ethylamine ARPs, with a drop in the IC_{50} values from 0.32–1.40 to 0.15–0.24 mg/mL. Even though the shorter, ethylamine ARP series displayed 20–70% cell viability after 24 h at a concentration of 1.0 mg/mL, this cytotoxic effect

was negligible in comparison to the effect of the tested antibiotic with an IC_{50} of 0.05 mg/mL. Hence, the therapeutic index (TI), relating antimicrobial effects to toxicity, was in favor of the polymeric materials. None of the samples displayed hemolytic activity. Furthermore, reduction of PEG content in the ARPs further increased toxicity.

3.5.2. Cross-linked SCNPs

Most cytotoxic studies on cross-linked SCNP are reported for SCNPs composed of biocompatible moieties, such as glycol or PEG. Likewise to the PEG ARPs, covalently cross-linked PEG SCNPs with degradable ester linkers had no significant effects at concentrations of up to 0.12 mg/mL on cell viabilities of HEK-293T cells within 1–3 days incubation [55]. Also, dextran and glycol methacrylate SCNPs, cross-linked via thiol-Michael addition, showed no discernible cytotoxic effects to HeLa cells after 48 h incubation at concentrations of up to 0.05 mg/mL and 0.2 mg/mL, respectively [52, 76]. Even modifying the dextran with a Tn antigen moiety did not affect metabolic activity or morphology of HeLa cells [80]. Glycol SCNPs were further tested on human brain endothelial cells, hCMEC/D3, and neither cell viability, nor cell morphology was noticeably influenced by incubation with the particles. As described above, the group of Zimmerman investigated the cellular uptake behavior of differently sized and glycol modified polyolefin SCNPs prepared by ring-opening and ring-closing metathesis [73–75, 85]. The observed cell-uptake to HeLa cells did not influence their viability considerably. Furthermore, different surface modified particles were tested on human liver cancer HepG2 cells and cell viabilities also remained above 80% at concentrations up to 15 μM for all samples (0.3–0.4 mg/mL) [74]. Even the copper-complexing SCNPs had only moderate effects on HEK-293 and MDA-MB-231 cells [85]. Despite minimal toxicity, a hydrogen peroxide assay revealed production of peroxides, presumable due to the copper in the SCNPs. Additionally, a hemolytic activity study did not show any unexpected hemolytic behavior of the SCNPs.

A detailed study into the cytotoxic effects of diamine cross-linked poly(*N*-phenyl)/acrylamide/acrylic acid SCNPs as potential protein mimic of ocular lens crystallins was conducted via electric cell-substrate impedance sensing (ECIS), which allows real-time measurement of cell monolayer resistance [99]. SCNPs incubated at concentrations of 0.1–30 mg/mL with primary porcine retinal epithelial cells (ppRPE) and with primary porcine lens epithelial cells (ppLE) were tracked over 6 days. These rather high concentrations were chosen to evaluate SCNPs as lens material with aimed concentrations of 300 mg/mL. Effects on ppRPE cell were noticeably dependent on nanoparticle concentration. Concentrations above 1 mg/mL resulted in reduced resistance at every evaluated time point, implying toxic effects, although up to concentrations of 5 mg/mL, cells continued to grow. At higher concentrations, cell growth stagnated, with full cell death observed after 6 days at 30 mg/mL. Microscopy images supported the particles' influence on cell morphology for concentrations of 15 mg/mL and higher after 6 days of incubation. ppLE cells were not nearly as much influenced by the SCNPs, with cell resistance reducing only at concentrations of 15 mg/mL and higher. Considering the high concentrations evaluated here and the presence of primary amines on the SCNPs, cytotoxicity was comparably low and only noticeable after prolonged exposure. Furthermore, ECIS online measurements were shown to give a more complete insight into the cell behavior and represent an interesting alternative characterization technique for cell viability, in comparison to mere metabolic activity assays, which are invasive and only represent the cell status at explicit time points.

So far *in vivo* toxicity studies of SCNPs were limited by work of Loinaz and co-workers on poly(methacrylic acid) SCNPs [77]. After finding no noticeable effects on the viabilities of six pancreatic cell lines after 72 h of incubation with 0.2 mg/mL SCNPs, the particles were tested on mice via intravenous injection of 12.5 mg/kg, 25 mg/kg and 100 mg/kg of SCNPs. For 100 mg/kg, all three and for 12.5 mg/kg, one out of five mice had developed thrombosis at the injection side. Apart from small fluctuations in the concentrations of liver enzymes, other tissues and organs were not found to be affected after 24 h of nanoparticle exposure, and no change in behavior was reported.

Until now, these initial series of *in vitro* toxicity evaluations generally reveal only minimal toxicities that are primarily related to the presence of external contaminants, such as metal ions, or primary amines, which are known (and also designed) to cause toxicity. Nonetheless, *in vitro* evaluations are only the first step and additional detailed *in vivo* studies are required to gain a general understanding of SCNP-related toxicity, especially as long-term and accumulative effects of such nanoparticles are still unknown. Consequently, evaluation studies should consider the aspect of size.

4. Medical application of SCNPs

The number of potential applications for SCNPs is increasing rapidly – ranging from antimicrobial agents [140], sensors [141, 142], protein storage [113], and eye lens implants [99]. As discussed in the previous section, SCNPs have been designed to exhibit promising characteristics in terms of biocompatibility, distribution and stability. In this section, the potential of water-soluble SCNPs in medical applications will be discussed in view of the findings in Section 3.

4.1. Biodistribution

Almost a magnitude smaller than conventional polymer nanoparticles, their size is the most prominent feature of SCNPs with the potential of unique *in vivo* behavior. Via SPECT, 15-nm-sized ^{67}Ga-chelating dextran SCNPs (13 nm in diameter in TEM) were detectable in the lungs directly after pulmonary administration of the aerosol to rats and ^{67}Ga-chelating poly(methacrylic acid) SCNPs (15 nm in diameter in TEM) have been found mainly in the liver and in the bladder, but also in tumor tissue after intravenous injection to a pancreatic cancer mouse model (Fig. 9) [52, 77]. However, detailed biodistribution studies for SCNPs are still lacking.

4.2. SCNPs as drug delivery systems

4.2.1. Encapsulation & release of cargos

In order to use polymer nanoparticles as drug delivery vehicles, drugs may be either linked to the particle or encapsulated. Sensor (dye) molecules, such as Reichardt's dye [91], pyrene [64], Nile red [64, 106], and naphthalimide [109], have been encapsulated into SCNPs to evaluate the encapsulation process. Further, encapsulation of a number of different therapeutic cargos has been demonstrated, including vitamin B_9 [46, 143], and 5-fluorouracil [103]. The cargos are commonly directly added to the reaction mixture during the SCNP formation process and randomly entrapped, often supported by hydrophobic interactions. Modern SCNP preparation methods allow concentrations of up to 100 mg/mL during the formation, which facilitates passive encapsulation processes [55]. Solvatochromic properties of dyes, such as Nile red, are highly suited for monitoring hydrophilicity inside particles. Addition of the hydrophobic dye Nile red to self-folding PEG/BTA ARPs resulted in a blue shift in the emission spectrum, which was interpreted as evidencing the presence of hydrophobic pockets inside the folded ARPs [106]. Likewise, a naphthalimide-based dye, as well as Reichardt's dye were employed to verify folding of PEG/Jeffamine ARPs [57, 91, 109].

The encapsulation of molecules inside ARPs has also been utilized to entrap drug molecules and drug models. The fragrants terpinyl acetate (0.1 wt%), R-limonene (0.5 wt%) and 4-anisaldehyde (1.0 wt%, no phase separation observed) were separately added to pVAc grafted PEG ARP until phase separation occurred [98]. Successful encapsulation was concluded from a decreased cloud point and from particle swelling as observed by DLS. ARP sizes increased from 22 nm in diameter to 52 nm in the case of anisaldehyde, which was related to the decreased

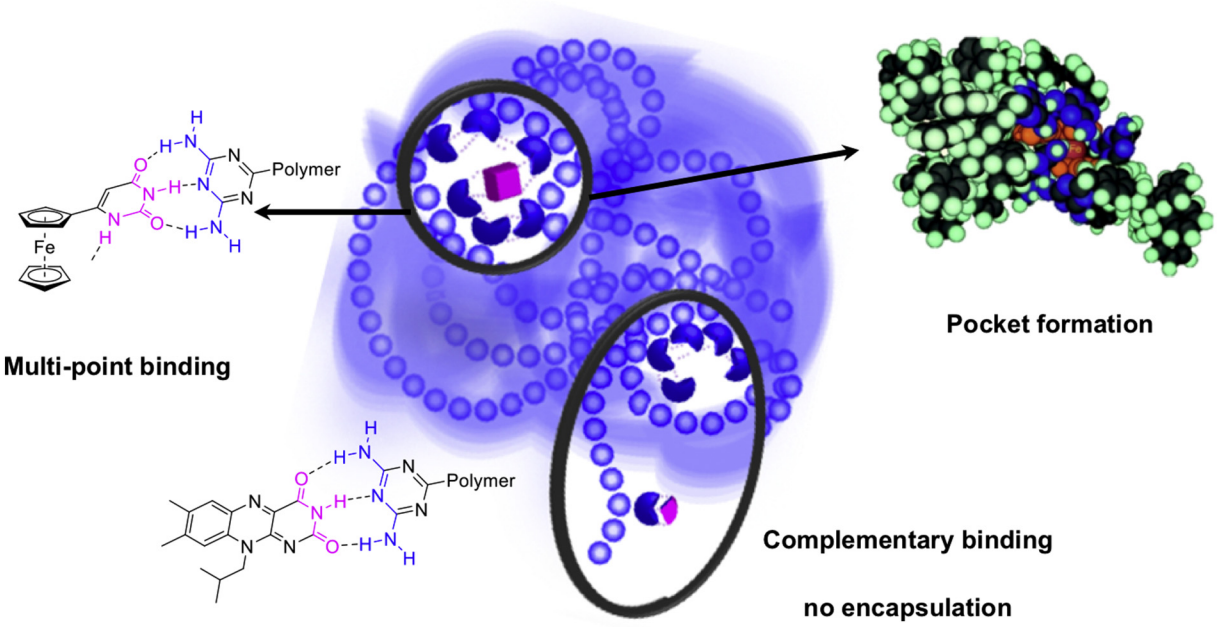

Fig. 6. Schematic representation of supramolecular recognition of 6-ferrocenyluracil (4-point hydrogen binding guest) and flavin (complementary hydrogen bonding motif) in diaminotriazine folded nanoparticles. Adapted from ref. [146] with permission of American Chemical Society (2000).

hydrophobicity, allowing the entrapped molecules to be located closer to the outside of the SCNPs. Sato and co-workers concluded from their SAXS experiments on self-folded ionic ARPs that 1-dodecanol, despite being hydrophobic, locates in the intermediate section of the particle, between core and outside [144].

Likewise, drug loading with the hydrophilic chemotherapeutic 5-fluorouracil changed the size of PEG U-DPy ARPs from 20-nm- to 100-nm-sized vesicles as observed by DLS and TEM measurements [103]. Drug loading of up to 19.6 wt% was achieved and a combination of high temperature and low pH was needed to break the U-DPy hydrogen bonds and thus to release the drug in water. Whereas at 37 °C and pH 4 only 20% of the drug was released, 91% of the drug was released at 47 °C. The authors suggest application of these ARP drug delivery systems in chemotherapy as cancer tissues provide a more acidic environment and (slightly) elevated temperatures.

For intramolecularly folded diaminotriazine styrene based SCNPs, the competitive binding mechanism with small molecules by complementary hydrogen motifs and π-stacking was studied in apolar solvents by ^{1}H NMR spectroscopy (Fig. 6) [145, 146]. Whereas flavin with a 3-point hydrogen binding site revealed only a low association constant of 36 M^{-1} in titration experiments, which was assigned to competitive binding accompanied by unfolding the assembled polymer, the electroactive 6-ferrocenyluracil, endowing a 4-point hydrogen binding side, showed an over 13-fold increased association constant, interpreted as favorable for internalization of the compound. This way of encapsulation even prevented precipitation of oxidized ferrocenium during cyclic voltammetry experiments.

Covalently cross-linked methacrylate SCNPs, containing 41 wt% of vitamin B_9 (i.e. folic acid), were obtained by Michael addition cross-linking [46]. As these particles are not water-soluble, they were placed into water to release the entrapped drugs. Release took 5–6 h and comparison with the power law model specified release by Fickian diffusion [147]. In another study, folic acid was loaded together with the potential anti-cancer drug hinokitiol with a total drug load of 51 wt %, corresponding to 170 molecules of folic acid and 410 molecules of hinokitiol per nanoparticle [147]. When testing the combined release of both drugs at pH 6 and 8, initial, burst release was slightly faster at pH 8, but the total release took 4 h for both conditions (Fig. 7).

Disulfide-linked SCNPs were loaded separately with pyrene and Nile red (each 1 wt% in methanol) [64]. Low amounts of DTT used to create free thiols for nanoparticle formation and the particles were stable up to 5 μM DTT with no significant amount of Nile red releasing. However, at higher DTT concentrations (5 mM), disulfide bridges were cleaved, and Nile red was released when dialyzing the particles in water (Fig. 8). After 24 h, release stagnated with 89% of the dye released. Hence, release from SCNPs is not limited to passive diffusion alone, but can also be in response to for example a reducing environment. Related work on disulfide nanogels showed the potential of these materials in doxorubicin encapsulation and intracellular delivery [89].

Nile red was also encapsulated in covalently cross-linked glycol methacrylate SCNPs [76]. Shifts in the fluorescence spectra of Nile red and increased solubility in water confirmed encapsulation. Importantly, SCNP loading could be performed both in organic as well as aqueous environment, offering new ways for polarity-independent drug encapsulation. Confocal microscopy suggested co-delivery of particles and cargo to hCMEC/D3 cells. Additionally, the antibiotic Rifampicin was encapsulated and in a subsequent dialysis study to water, release of Rifampicin from SCNPs was decelerated as compared to free Rifampicin.

After demonstrating successful coupling of a lysozyme to PEG ARPs via disulfide and NHS coupling, Sawamoto and Maynard and co-workers also presented encapsulation of proteins in fluorous PEG ARPs [113, 148]. Two model proteins, lysozyme and α-chymotrypsin, were lyophilized, dispersed in *2H,3H*-perfluoropentane (HPFP) and, after 24 h, extracted back to the aqueous phase in the presence and absence of fluorous PEG ARPs. Circular dichroism (CD) spectroscopy and enzyme activity studies revealed that the proteins remained stable when in the presence of ARPs. Surprisingly, α-chymotrypsin remained active with the ARPs in HPFP, whereas storage in water alone decreased its activity significantly. In case of dissolving the proteins/ARP in chloroform instead of HPFP, the perfluorinated PEG ARPs were no longer able to protect the enzymes and activity was lost, underlining the importance of the amphiphilicity of the ARPs in protecting the proteins. Accordingly, ARPs are suitable in stabilizing and protecting enzymes in organic solvents and could be of use for protein storage. Furthermore, the fluorous ARPs are also anticipated to act as oxygen carriers, as

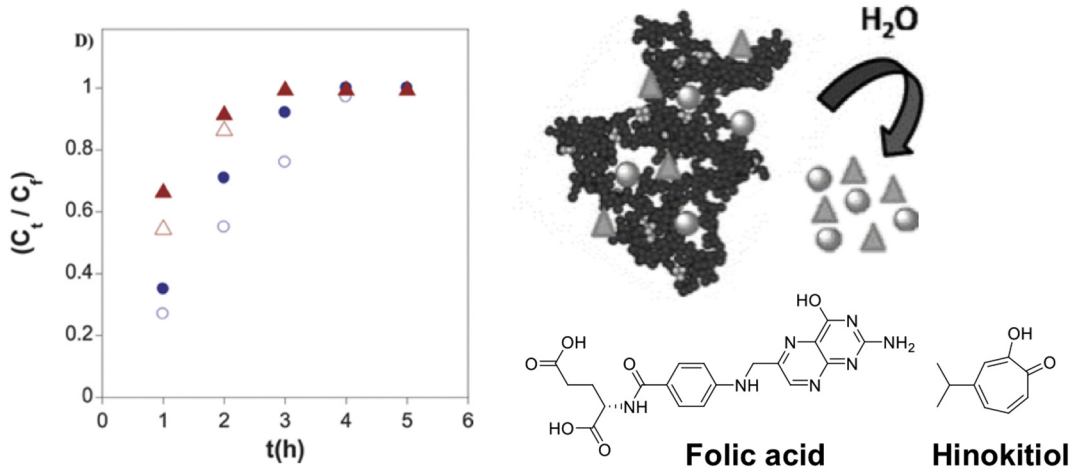

Fig. 7. Simultaneous release of folic acid (open symbols) and hinokitiol (filled symbols) from MMA SCNPs to water at pH 6 (blue) and pH 8 (red) (C_t = concentration of drug released at time t, C_f = total concentration of drug released). Adapted from ref. [143] with permission of John Wiley Sons, Inc. (2016).

fluoropolymers are known to efficiently dissolve oxygen [113, 149].

Overall, drug encapsulation with rather high drug loading and, in combination with passive and triggered release, has been demonstrated for SCNPs [64, 76, 103]. Likely, hydrophobic interactions will facilitate the encapsulation of hydrophobic drug, especially for self-assembled SCNPs. Even so, Nile red was efficiently encapsulated in SCNPs in water, as well as in organic solvent.

4.2.2. Prospected applications

Besides encapsulation, drugs may also be coupled to nanoparticles, either with retention of their reactivity or through a degradable linker. Proteins were conjugated onto fluorous PEG ARPs via disulfide bridges and NHS ester coupling for targeting purposes, in which oxygen was proposed as a cargo for the fluorophilic core [113]. Both therapeutic and targeting peptides have been conjugated onto SCNPs in a post-formation step [70, 77]. In the first case, a model peptide was coupled to SCNPs by a disulfide bridge that appeared to be cleaved in the cellular environments, whereas a guanidine dendritic unit was irreversibly added by thiol-Michael addition as targeting moiety. In the latter, PTR86, a peptide with high affinity to receptors overexpressed in pancreatic tumors, was covalently bound to radiolabeled SCNPs. SPECT-CT imaging revealed that the particles mainly accumulated in the liver 3 h after intravenous administration (Fig. 9). Further, the ratio of the distribution between tumor and muscle tissues was regarded. Interestingly, even the non-targeted particles accumulated in tumor tissues to comparable extents as the targeted SCNPs within 24 h, which was assigned to the enhanced permeability and retention (EPR) effect. After 48 h, however, the amount of targeted SCNPs in the tumor side increased, resulting in a significantly higher amount than the non-targeted controls.

Above mentioned examples demonstrate the applicability of SCNPs as drug delivery platform in combination with targeting moieties. Small particles are generally rapidly cleared from the body, hence, the time frame is designated to rather short applications. However, integration of SCNPs in degradable hydrogel scaffolds to tune the release profile of SCNPs could broaden this application window. Fulton and co-workers demonstrated for SCNPs with dynamic covalent cross-links reversible switching between SCNP and hydrogel state by temperature changes [12].

Dynamically cross-linked carbohydrate SCNPs were also investigated in film formation with molecular recognition motifs [62]. The authors suggested for these dynamically cross-linked films applications of covering 3D surfaces such as bacteria, virus, or also artificial surfaces. In a similar fashion, Barner-Kowollik and co-workers coated mannose-based covalently cross-linked SCNPs on nanodiamonds of 100 nm, which are themselves considered as potential drug delivery and imaging systems [61, 150]. Nanodiamonds decorated with fluorescent mannose SCNPs were incubated with RAW 64.7 macrophage cells, which are known to express mannose receptors. Fluorescent signal was observed by confocal microscopy in the cytosol without reduction of the cell viability at 0.1 mg/mL. Both examples represent how carbohydrate SCNPs can be applied to cover surfaces and hence provide

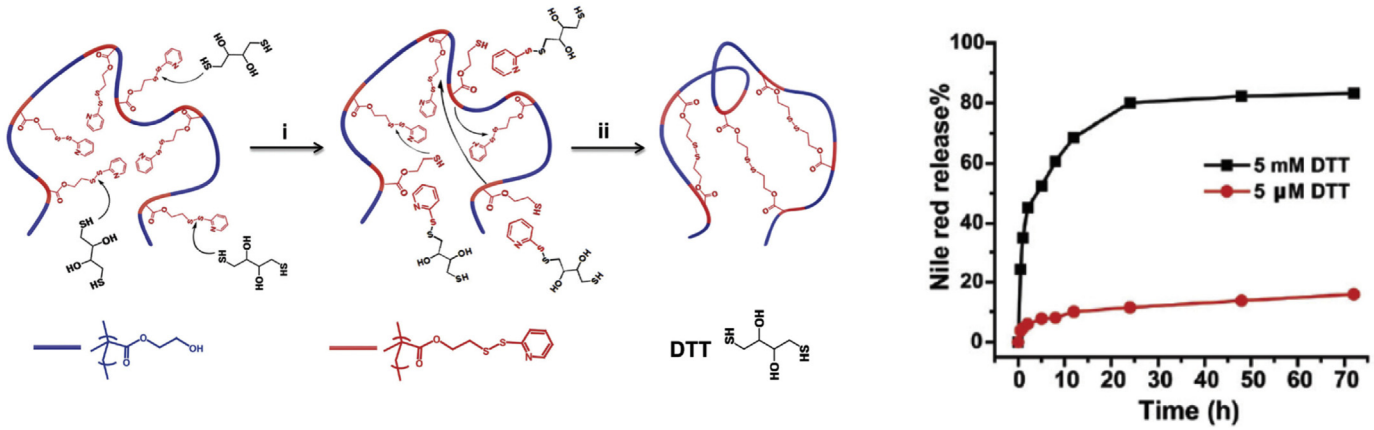

Fig. 8. a) Schematic representation of SCNP formation by thiol-disulfide exchange; b) release from disulfide SCNPs of entrapped Nile red at different 5 μM and 5 mM DTT. Reproduced with permission from ref. [64] with permission of The Royal Society of Chemistry (2015).

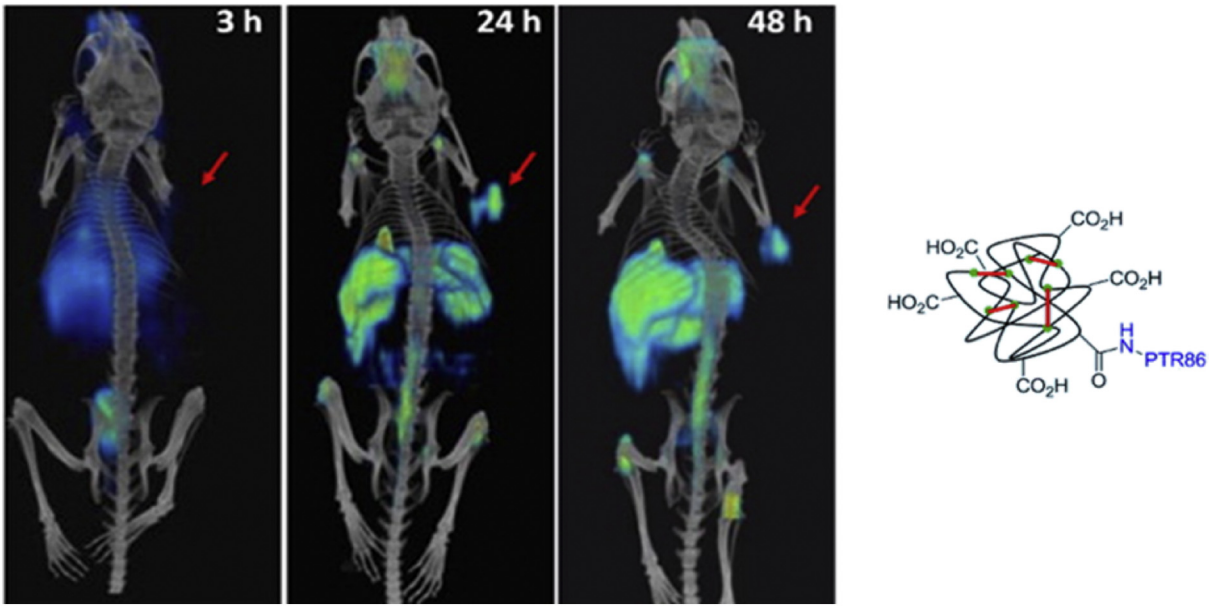

Fig. 9. SPECT-CT images of pancreatic tumor mice injected with Ga^{67} labelled carboxylic acid SCNPs that are targeted against pancreatic cancer (recorded 3 h, 24 h, and 48 h after injection). The red arrows point to the tumor site. Reproduced with permission from ref. [77]. with permission of American Chemical Society (2016).

them with biological function such as targeting.

4.3. SCNPs as drug conjugates

Next to encapsulation or conjugation of drugs, the polymer itself can also act as a drug [151, 152]. For example, the anti-inflammatory effect of glatrimer acetate (Copaxone®), a random copolymer based on four amino acids, is applied in the treatment of multiple sclerosis [153]. However, many applications of polymeric drugs are targeted against the membranes of bacteria and viruses. In case of SCNPs, amine containing PEG ARPs, which were inspired by the structure of amphiphilic, antimicrobial peptides, showed antimicrobial activity to *Pseudomonas aeruginosa* and *E.coli* strains [140]. The authors correlated increased hydrophobicity of the ARPs with the membrane disruption efficiency towards gram negative bacteria. Although less efficient than the compared antibiotics (colistin), cytotoxic effects on rat liver cells were decreased, resulting in a better therapeutic index (TI) for the ARP SCNPs, which are assumed to disrupt the membranes. Similar to reference antibiotics, strains developed resistance to the ARPs after several days, which is a commonly observed problem with antibiotics. Further, the ARPs were tested against biofilms, which are usually formed by microorganisms on surfaces. Within 1 h, the bacteria were killed by the tested ARPs and most strikingly, the films were dispersed. This was in strong contrast to colistin, which did not disperse the film within that time and even resulted in further increased biofilm mass. Consequently, these SCNPs could find application, where common antibiotics fail.

Differently, α-Tn antigen mimetic moiety was coupled to dextran SCNPs to trigger immune-responses similar to immune proteins on human PBMC cells [80]. Since the α-Tn antigen is a tumor-associated carbohydrate antigen (TACA) and hence overexpressed in cancer cells, it is under investigation as anticancer vaccine. However, the native antigen has limitations in terms of stability and antibody response. The immune response of the targeted nanoparticles in human peripheral blood mononuclear (PBMC) cells was investigated. Like the positive controls, the targeted particles triggered cross-talk between Tn-antigen receptors as observed by upregulation of interleukin-6 and -10. Non-targeted SCNPs did not stimulate secretion of the interleukins. Therefore, SCNPs decorated with α-Tn antigen mimetic offer a promising alternative to vaccine proteins.

4.4. SCNPs as imaging agent

For *in vivo* imaging agents a wide distribution in the body is desirable, without long-term accumulation, while ensuring stability and contrast of the label remains highly important.

Odriozola and co-workers investigated a Gd(III)-chelating cross-linker for SCNP as MRI contrast agent [8]. After SCNP formation, the cross-linkers were still accessible for the paramagnetic Gd ions and decreased relaxation times in comparison to commercial MRI contrast agents were found. However, in terms of relaxivity SCNPs did not outperform other Gd(III)-containing macromolecules. Comparable relaxivity values were obtained from semiconducting SCNPs with catechol moieties for Gd(III)-chelation developed by Harth and co-workers [72]. These semi-conducting SCNPs further display fluorescent properties with an increased quantum efficiency upon SCNP formation (5.1%) enabling multimodal imaging. By intramolecular cross-linking, the luminescence properties improved as compared to a linear precursor, attributed to site-isolation effects. Similarly, conjugated polyelectrolyte ARPs achieved quantum yields of 26% [154]. In this process, single-chain aggregates exhibited elongated fluorescence lifetimes and increased quantum yields in comparison to multi-chain structures.

Also, Loinaz and co-workers utilized SCNPs with the ^{67}Ga(III)-chelating moieties, DTPA and NODA, for SPECT-CT *in vivo* imaging [52, 77]. Whereas SPECT was used to monitor the distribution of the radiometal, CT provided anatomical information of the tested rodents. With radiolabeling efficacy of 50–60%, dextran SCNPs were visualized in rat lungs and targeted carboxylic acid SCNPs were tracked in a pancreatic cancer mouse model [77]. Although the authors found appreciable stabilities of the radiolabeling (< 90%), detachment of the radiometal needs to be taken into account.

Further, SCNPs have also been used as template for size-controlled formation of QDs [71, 155] and gold nanoparticles [66, 156], which introduce luminescence properties and contrast to the nanoparticles with potential (medical) imaging applications [157–159]. Modification of the SCNPs with DNA led to gold nanoparticles attached with a single DNA strang [156]. Hence, SCNPs might be used as QD-like material or as nanoreactors for such, but also to introduce in a controlled manner functional moieties onto metal particles, for example for targeting purposes.

4.5. Protein mimicry

4.5.1. Protein structure

When considering proteins as self-folding dynamic polymers where the assembly process is driven by hydrophobic interactions, ARPs approach the protein assembly process most closely. However, in order to provide functionality, site-specificity is required to define the SCNP structure. In proteins, such structural control starts with the primary structure. The development of powerful controlled radical polymerization techniques has enabled the preparation of polymers with excellent control over molecular weight and narrow polydispersities, more closely approximating protein monodispersity [160]. As the amino acid sequence determines a protein's secondary structure, characterized by non-covalent folding motifs, which in turn gives way to the tertiary structure, recent efforts are focusing on achieving sequence control in polymers [161–165]. By positioning the cross-linkable groups in a polymer, intramolecular point-folding leads to differently shaped SCNPs [166]. Through substitution of positioned pentafluorophenol moieties in polystyrene copolymers with cysteine moieties, intramolecular cross-linking via disulfide bonds was achieved [167]. Combining this approach with disulfide bridged SCNPs in water, would resemble the assembly process of the tertiary structure of proteins [64]. In order to further add sequence control to SCNPs, Berda and coworkers cross-linked a styrene random copolymer with a sequence-defined cross-linking technique, i.e. isocyanide-based multicomponent reaction (IMCR), resulting in depsipeptide and dipeptide linkages in the polymer [168]. In case of dipeptide linkages, intramolecular interactions were observed, presumably as a result of hydrogen bonding.

The secondary structure of proteins is determined by intramolecular supramolecular folding motifs such as α-helices and β-sheets. Folding of triblock copolymer SCNPs by π-π interactions between styrene and pentafluorostyrene blocks in chloroform under high dilution, was compared with a β-hairpin motif, introducing secondary structures to SCNPs. Alternatively, folding of PEG ARPs in water via self-structuring of chiral BTA moieties, resulted in a Cotton effect in CD measurements, related to chiral helical aggregates [16, 23]. Additionally, free fluorescently labeled BTA-molecules were also incorporated into BTA-assembly inside the SCNPs [169]. In combination with ruthenium(II)-coordinating diphenylphosphino-functional styrene, PEG BTA ARPs formed hydrophobic pockets that allowed ruthenium(II)-catalyzed oxidations in water [16, 107]. As such, aided by L-proline moieties, PEG BTA ARPs mimicked the catalytic properties of aldolase enzymes in water [105, 169]. A later study revealed that the BTA moieties are not essential to forming the pockets in ARPs, but rather the balance between hydrophobic and hydrophilic moieties was crucial [106].

Among other factors, hydrophobic pockets in the protein are crucial for enzymatic activity. In this respect, the inner structure of SCNPs plays a significant role. Whereas globular SCNPs are expected to form single, large compartments, sparse SCNPs are expected to exhibit several, individual pockets [101, 170]. Since a multitude of interactions determines the overall structure of proteins, controlled orthogonal multistep folding was investigated in SCNPs. Dimerization of the hydrogen-bonding unit, i.e. Hamilton wedge (HW)/cyanuric acid (CA) proved to be orthogonal towards thymine (THY)/diaminopyridine (AD) dimerization for dual point single-chain folding [171, 172] and towards crown ether/cation host-guest interactions in a multi-block copolymer (Fig. 10a) [173]. Likewise, BTA and photo-sensitive protected UPy-moieties were combined in an ABA block copolymer, resulting in stepwise polymer folding, with BTA-units providing helical assemblies and light-induced UPy folding giving rise to sheet-like assemblies [14]. Moreover, as the blocks were individually folded, compartments were created within the SCNP, as visualized by AFM (Fig. 10b). Likewise, combining BTA and HW-CA dimerization in an ABC block copolymer, enabled orthogonal self-assembly into SCNPs containing α-helix and β-sheet mimics [174]. However, apart from BTA folding, none of these strategies were demonstrated in water, most likely due to water interacting with (and disrupting) the hydrogen bonding motifs.

An example of covalent orthogonal folding was demonstrated via sequential folding of an anhydride functional polyolefin via nucleophilic addition of diamine and subsequent thiol-ene "click" reaction with a dithiol, as well as by Michael reaction of methyl methacrylate based copolymers with sequential metal complexation [119, 175]. Interestingly, multi-folding resulted in smaller, more spherical SCNPs [120]. Independently, sequential collapse of a ABC block copolymer containing pentafluorophenol and alkyne moieties via cross-linking through diamine substitution and through Eglinton alkyne dimerization, led to two distinct compartments within the SCNPs [176]. In nature, the consecutive addition of amino acids by the ribosome influences the folding of proteins. Similarly, Zhang *et al.* alternated RAFT copolymerization and intramolecular isocyanate cross-linking to achieve three individual subdomains (Fig. 11) [88]. ^{1}H-NMR spectroscopy and SEC analysis suggested hydrogen-bonding interactions caused by urea and amine functions assisted the cross-linking.

UV cross-linking of a diluted diblock copolymer in the presence of a L-phenylalanine anilide (L-PheA) template, yielded tadpole-type SCNPs with high binding affinity for L-PheA as opposed to the D-isomer [26]. The so-called chiral imprinting offers a further possibility of inducing specific binding and catalytic cavities inside to polymer particles.

Most of the mentioned examples of orthogonal folding and compartmentalization were carried out in organic solvent; in particular when hydrogen bonding motifs were employed. Recently, orthogonal folding of a ABC HPMAA block copolymer in water was shown by two blocks that both complexate copper(II), yielding SCNPs with two distinct domains [84]. Whereas copper coordination with the imidazolium block is relatively pH independent, the folding of the second, quaternary ammonium block is pH responsive. Therefore, the SCNP architecture is pH dynamic as observed also in natural proteins.

4.5.2. Approaching natural proteins

Combining sequence-control, self-recognizing motifs, point folding and orthogonal cross-linking enables carefully modeling SCNPs into well-defined, protein-like structures. However, even intrinsically disordered proteins are not without function and thus, structure definition may not always be necessary. Moreover, the protein-like appearance of polymers is readily endowed with amino acid functionalities. This can be achieved either by post-formation functionalization of particles with amino acids/peptides or by directly applying amino acid-like monomers in the preparation of precursor polymers. An example of this approach is the case of phenylalanine grafted γ-PGA ARPs [43, 60]. The resulting SCNPs featured hydrophobic domains as detected by the emission of pyrene. Interestingly, cross-linked (*N*-phenyl)/acrylamide/acrylic acid SCNPs were investigated to match optical and mechanical properties of β-crystallins, i.e. globular structural proteins in the lens and cornea of the eye, and to serve as an ingredient for eye lens implants as replacement of aggregated crystallins in case of cataract [99]. In a different fashion, SCNPs approximated glyco-proteins by equipping them with carbohydrate functionalities, either post-formation or by applying glycomonomers [62, 80]. These glyco-SCNPs exhibited molecular recognition and triggered specific cell response.

4.5.3. Metallo-proteins & enzymes

Metal-coordinating proteins enable functionalities such as oxygen binding in the case of porphyrin-Fe(II) coordination in hemoglobin. Addition of protein-like moieties, such as the mono-addition of an azadithiolate-bridged Fe_2S_2 unit, which is based on the active site of [Fe-Fe] hydrogenase to poly(styrene-*co*-methacrylate) SCNPs, highlights the potential of enzyme mimicry (Fig. 12a) [177]. A type of binding pocket, composed of hydrogen bonding and π-stacking motifs, was created for encapsulation of 6-ferrocenyluracil in intramolecularly assembled diaminotriazine-functional polystyrenes (Fig. 5) [145, 146]. The combination of hydrophobic pockets and metal coordination may endow SCNPs with catalytic activities. For example, imitation of a

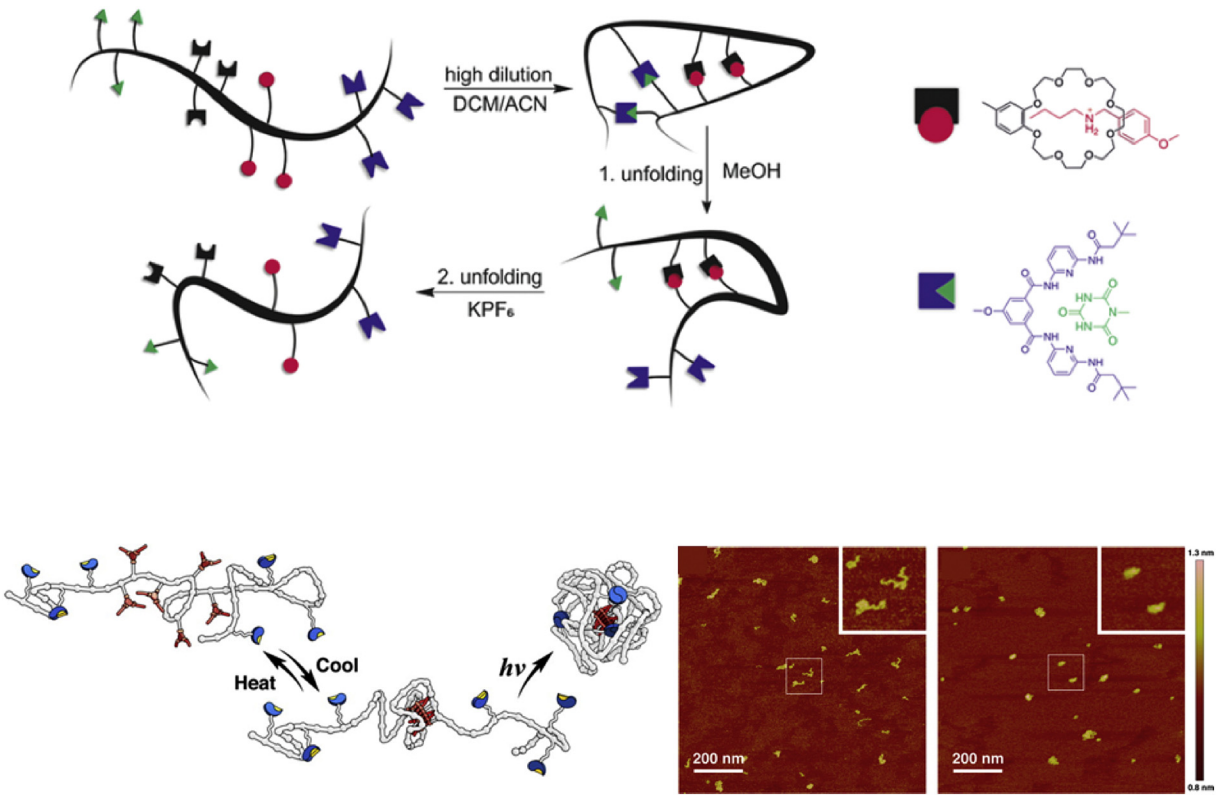

Fig. 10. Schematic representation of orthogonal folding of SCNPs a) by reversible Hamilton wedge (HW)/cyanuric acid (CA) dimerization and reversible host-guest interaction of benzo-21-crown-7 with a secondary alkylammonium salt; b) by BTA and UPy binding motifs. AFM images before (c) and after (d) light activation. a) Reproduced from ref. [173] with permission from John Wiley Sons, Inc (2016); b-d) reproduced from ref. [14] with permission from American Chemical Society (2013).

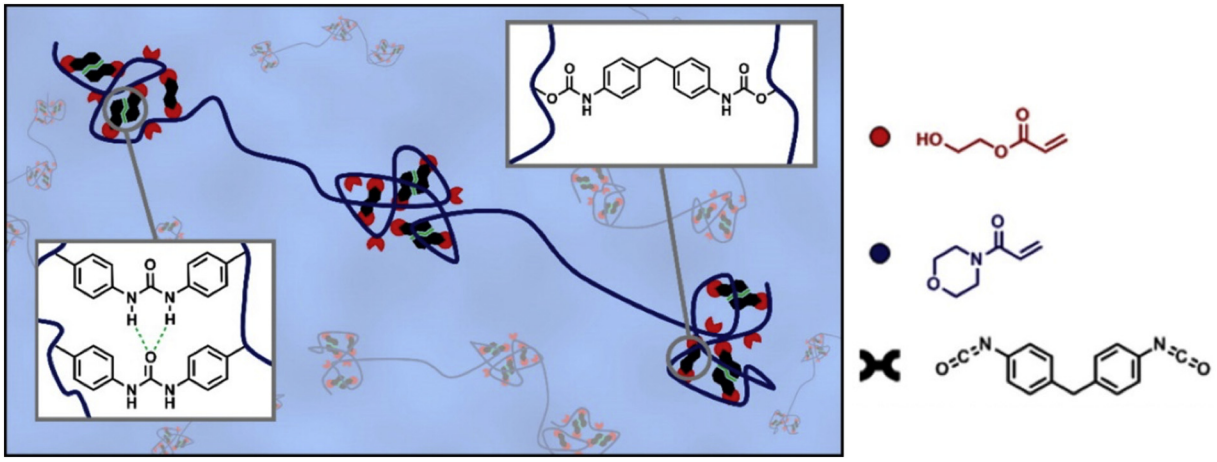

Fig. 11. Compartmentalization by sequential chain growth and intramolecular isocyanate cross-linking of HEA copolymers. Reproduced with permission from ref. [88] with permission of American Chemical Society (2016).

polymerase reaction was achieved with glycidyl methacrylate SCNPs bearing $B(C_6F_5)_3$, which catalyzed cationic ring opening polymerization, yielding for example polytetrahydrofuran [178]. Enzymatic activity of metal-coordinating SCNPs is a popular topic of research in the SCNP field and has been demonstrated for several metals as extensively reviewed elsewhere [170, 179, 180]. In contrast, in biologically relevant surroundings SCNP catalysis has been rarely exploited. The groups of Zimmerman and Palmans demonstrated copper and palladium catalysis by SCNPs in the cellular environment as discussed in Section 3.4. [85, 109]. In this context, also porphyrin SCNPs were developed for light-triggered singlet oxygen generation in cells [109]. Previously, Fe(III)-porphyrin star SCNPs were designed as an analogue of heme protein with preserved ligand binding and redox activity of the porphyrin group in a DMSO/water mixture (Fig. 12b) [181].

The numerous synthetic routes towards SCNPs provide increasing levels of control over molecular composition, dynamics, size, inner structure and morphology, offering a multitude of possibilities for preparing protein-like materials, and including functionalities in them such as catalytic activity, site-specific inhibitors and targeting properties. For further reading of polymer synthesis techniques for protein mimicry, the authors recommend a recent review by Berda and coworkers [180].

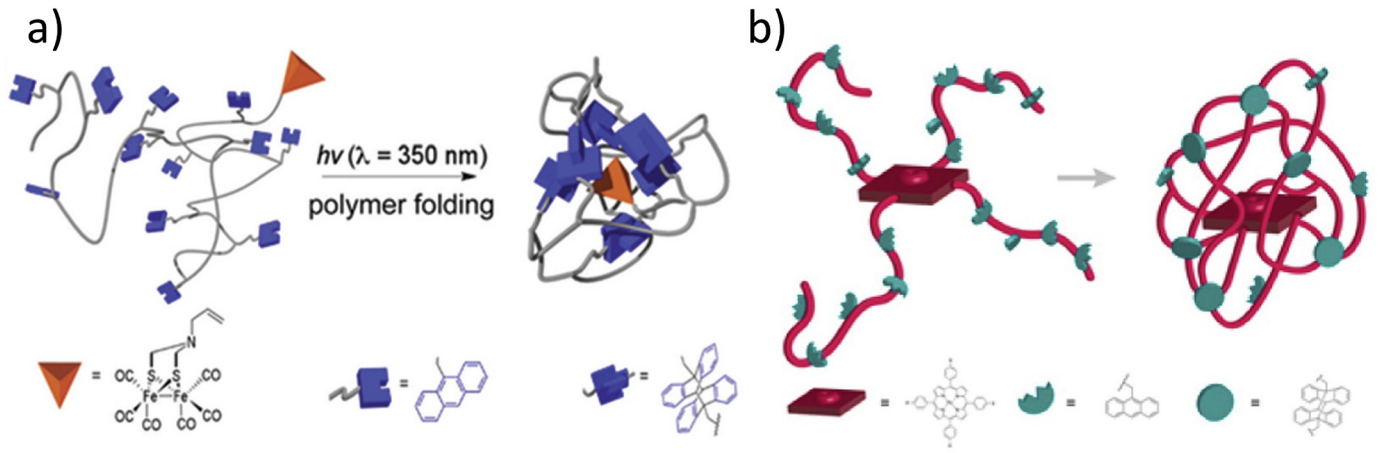

Fig. 12. Examples of incorporation of functional metal units into SCNPs as enzyme-mimics of a) hydrogenase and b) hemoglobin. Reproduced from [177] with permission of The Royal Society of Chemistry (2015) and from ref. [181] with permission of American Chemical Society (2016).

5. Conclusions

A tremendous toolbox of orthogonal chemistry is nowadays available for SCNP construction. Their size in particular, sets SCNPs in context with proteins and viruses, which is synthetically otherwise only achieved by dendrimer-like structures. Beyond that, SCNPs possess the tremendous variability of polymer chemistry, so that the question arises how to design SCNPs to suit (medical) applications, such as drug delivery and targeted imaging. SCNPs may provide comparable or enhanced therapeutic potential as existing polymer-based therapeutics, including polymer-drug candidates and bioactivity by the polymer itself. Definition of the 3-dimensional structure enables hydrophobic domains in water-soluble SCNP, which can not only be utilized for drug encapsulation, but also for catalytic activities. The structure of SCNPs is reminiscent of proteins and smart polymer design has brought mimicking of natural macromolecules within reach. Depending on SCNP design, initial toxicity evaluations attribute high biocompatibility to SCNPs and, depending on their size, extraordinary distribution behavior is prospected. Combining all this with targeting properties is a powerful approach towards new biomaterials. Systematic investigations into *in vitro* and *in vivo* behavior are, however, required in order to understand and predict biodistribution behavior, biocompatibility and drug release of SCNPs under realistic conditions, and to take full advantage of their potential.

Acknowledgements

We gratefully acknowledge funding from the Netherlands Organization for Health Research and Development (ZonMw, project number 733050304).

References

[1] M.K. Aiertza, I. Odriozola, G. Cabañero, H.-J. Grande, I. Loinaz, Single-chain polymer nanoparticles, Cell. Mol. Life Sci. 69 (2012) 337–346, https://doi.org/10.1007/s00018-011-0852-x.
[2] M. González-Burgos, A. Latorre-Sánchez, J.A. Pomposo, Advances in single chain technology, Chem. Soc. Rev. 44 (2015) 6122–6142, https://doi.org/10.1039/C5CS00209E.
[3] C.K. Lyon, A. Prasher, A.M. Hanlon, B.T. Tuten, C.A. Tooley, P.G. Frank, E.B. Berda, A brief user's guide to single-chain nanoparticles, Polym. Chem. 6 (2015) 181–197, https://doi.org/10.1039/C4PY01217H.
[4] S. Mavila, O. Eivgi, I. Berkovich, N.G. Lemcoff, Intramolecular cross-linking methodologies for the synthesis of polymer nanoparticles, Chem. Rev. 116 (2016) 878–961, https://doi.org/10.1021/acs.chemrev.5b00290.
[5] E. Harth, B. Van Horn, V.Y. Lee, D.S. Germack, C.P. Gonzales, R.D. Miller, C.J. Hawker, A facile approach to architecturally defined nanoparticles via intramolecular chain collapse, J. Am. Chem. Soc. 124 (2002) 8653–8660, https://doi.org/10.1021/ja026208x.
[6] T.E. Dukette, M.E. Mackay, B. Van Horn, K.L. Wooley, E. Drockenmuller, M. Malkoch, C.J. Hawker, Conformation of intramolecularly cross-linked polymer nanoparticles on solid substrates, Nano Lett. 5 (2005) 1704–1709, https://doi.org/10.1021/nl050941f.
[7] A.R. de Luzuriaga, N. Ormategui, H.-J. Grande, I. Odriozola, J.A. Pomposo, I. Loinaz, Intramolecular click cycloaddition: an efficient room-temperature route towards bioconjugable polymeric nanoparticles, Macromol. Rapid Commun. 29 (2008) 1156–1160, https://doi.org/10.1002/marc.200700877.
[8] I. Perez-Baena, I. Loinaz, D. Padro, I. García, H.-J. Grande, I. Odriozola, Single-chain polyacrylic nanoparticles with multiple Gd(III) centres as potential MRI contrast agents, J. Mater. Chem. 20 (2010) 6916, https://doi.org/10.1039/c0jm01025a.
[9] A. Sanchez-Sanchez, I. Asenjo-Sanz, L. Buruaga, J.A. Pomposo, Naked and self-clickable propargylic-decorated single-chain nanoparticle precursors via redox-initiated RAFT polymerization, Macromol. Rapid Commun. 33 (2012) 1262–1267, https://doi.org/10.1002/marc.201200180.
[10] A.E. Cherian, F.C. Sun, S.S. Sheiko, G.W. Coates, Formation of nanoparticles by intramolecular cross-linking: following the reaction progress of single polymer chains by atomic force microscopy, J. Am. Chem. Soc. 129 (2007) 11350–11351, https://doi.org/10.1021/ja0743011.
[11] B.T. Tuten, D. Chao, C.K. Lyon, E.B. Berda, Single-chain polymer nanoparticles via reversible disulfide bridges, Polym. Chem. 3 (2012) 3068, https://doi.org/10.1039/c2py20308a.
[12] D.E. Whitaker, C.S. Mahon, D.A. Fulton, Thermoresponsive dynamic covalent single-chain polymer nanoparticles reversibly transform into a hydrogel, Angew. Chem. 52 (2013) 956–959, https://doi.org/10.1002/anie.201207953.
[13] E.J. Foster, E.B. Berda, E.W. Meijer, metastable supramolecular polymer nanoparticles via intramolecular collapse of single polymer chains, J. Am. Chem. Soc. 131 (2009) 6964–6966, https://doi.org/10.1021/ja901687d.
[14] N. Hosono, M.A.J. Gillissen, Y. Li, S.S. Sheiko, A.R.A. Palmans, E.W. Meijer, Orthogonal self-assembly in folding block copolymers, J. Am. Chem. Soc. 135 (2013) 501–510, https://doi.org/10.1021/ja310422w.
[15] T. Mes, R. van der Weegen, A.R.A. Palmans, E.W. Meijer, Single-chain polymeric nanoparticles by stepwise folding, Angew. Chem. 50 (2011) 5085–5089, https://doi.org/10.1002/anie.201100104.
[16] T. Terashima, T. Mes, T.F.A. de Greef, M.A.J. Gillissen, P. Besenius, A.R.A. Palmans, E.W. Meijer, Single-chain folding of polymers for catalytic systems in water, J. Am. Chem. Soc. 133 (2011) 4742–4745, https://doi.org/10.1021/ja2004494.
[17] S. Mavila, C.E. Diesendruck, S. Linde, L. Amir, R. Shikler, N.G. Lemcoff, Polycyclooctadiene complexes of rhodium(i): direct access to organometallic nanoparticles, Angew. Chem. 52 (2013) 5767–5770, https://doi.org/10.1002/anie.201300362.
[18] A. Sanchez-Sanchez, A. Arbe, J. Colmenero, J.A. Pomposo, Metallo-folded single-chain nanoparticles with catalytic selectivity, ACS Macro Lett. 3 (2014) 439–443, https://doi.org/10.1021/mz5001477.
[19] T.A. Croce, S.K. Hamilton, M.L. Chen, H. Muchalski, E. Harth, Alternative o -quinodimethane cross-linking precursors for intramolecular chain collapse nanoparticles, Macromolecules 40 (2007) 6028–6031, https://doi.org/10.1021/ma071111m.
[20] J.B. Beck, K.L. Killops, T. Kang, K. Sivanandan, A. Bayles, M.E. Mackay, K.L. Wooley, C.J. Hawker, Facile preparation of nanoparticles by intramolecular crosslinking of isocyanate functionalized copolymers, Macromolecules 42 (2009) 5629–5635, https://doi.org/10.1021/ma900899v.
[21] A.R. de Luzuriaga, I. Perez-Baena, S. Montes, I. Loinaz, I. Odriozola, I. García, J.A. Pomposo, New route to polymeric nanoparticles by click chemistry using bifunctional cross-linkers, Macromol. Symp. 296 (2010) 303–310, https://doi.org/10.1002/masy.201051042.
[22] A. Sanchez-Sanchez, I. Pérez-Baena, J.A. Pomposo, Advances in click chemistry for single-chain nanoparticle construction, Molecules 18 (2013) 3339–3355, https://doi.org/10.3390/molecules18033339.

[23] J. Lu, N. ten Brummelhuis, M. Weck, Intramolecular folding of triblock copolymers via quadrupole interactions between poly(styrene) and poly(pentafluorostyrene) blocks, Chem. Commun. 50 (2014) 6225, https://doi.org/10.1039/c4cc01840k.
[24] G. Njikang, G. Liu, S.A. Curda, Tadpoles from the intramolecular photo-cross-linking of diblock copolymers, Macromolecules 41 (2008) 5697–5702, https://doi.org/10.1021/ma800642r.
[25] T. Terashima, T. Sugita, M. Sawamoto, Single-chain crosslinked star polymers via intramolecular crosslinking of self-folding amphiphilic copolymers in water, Polym. J. 47 (2015) 667–677, https://doi.org/10.1038/pj.2015.54.
[26] G. Njikang, G. Liu, L. Hong, Chiral imprinting of diblock copolymer single-chain particles, Langmuir 27 (2011) 7176–7184, https://doi.org/10.1021/la2006887.
[27] B.E.I. Ramakers, J.C.M. van Hest, D.W.P.M. Löwik, Molecular tools for the construction of peptide-based materials, Chem. Soc. Rev. 43 (2014) 2743, https://doi.org/10.1039/c3cs60362h.
[28] S.-D. Li, L. Huang, Pharmacokinetics and biodistribution of nanoparticles, Mol. Pharm. 5 (2008) 496–504, https://doi.org/10.1021/mp800049w.
[29] M. Longmire, P.L. Choyke, H. Kobayashi, Clearance properties of nano-sized particles and molecules as imagin agents: consideration and caveats, Nanomedicine 3 (2008) 703–717, https://doi.org/10.2217/17435889.3.5.703.
[30] D. Liu, A. Mori, L. Huang, Role of liposome size and RES blockade in controlling biodistribution and tumor uptake of GM1-containing liposomes, Biochim. Biophys. Acta 1104 (1992) 95–101, https://doi.org/10.1016/0005-2736(92)90136-A.
[31] W.H. De Jong, W.I. Hagens, P. Krystek, M.C. Burger, A.J.A.M. Sips, R.E. Geertsma, Particle size-dependent organ distribution of gold nanoparticles after intravenous administration, Biomaterials 29 (2008) 1912–1919, https://doi.org/10.1016/j.biomaterials.2007.12.037.
[32] G. Sonavane, K. Tomoda, K. Makino, Biodistribution of colloidal gold nanoparticles after intravenous administration: effect of particle size, Colloids Surf. B: Biointerfaces 66 (2008) 274–280, https://doi.org/10.1016/j.colsurfb.2008.07.004.
[33] E.A. Sykes, Q. Dai, C.D. Sarsons, J. Chen, J.V. Rocheleau, D.M. Hwang, G. Zheng, D.T. Cramb, K.D. Rinker, W.C.W. Chan, Tailoring nanoparticle designs to target cancer based on tumor pathophysiology, Proc. Natl. Acad. Sci. 113 (2016) E1142–E1151, https://doi.org/10.1073/pnas.1521265113.
[34] F. Zhang, J. Trent Magruder, Y.-A. Lin, T.C. Crawford, J.C. Grim, C.M. Sciortino, M.A. Wilson, M.E. Blue, S. Kannan, M.V. Johnston, W.A. Baumgartner, R.M. Kannan, Generation-6 hydroxyl PAMAM dendrimers improve CNS penetration from intravenous administration in a large animal brain injury model, J. Control. Release 249 (2017) 173–182, https://doi.org/10.1016/j.jconrel.2017.01.032.
[35] J.A. Pomposo, I. Perez-Baena, L. Buruaga, A. Alegría, A.J. Moreno, J. Colmenero, On the apparent SEC molecular weight and polydispersity reduction upon intramolecular collapse of polydisperse chains to unimolecular nanoparticles, Macromolecules 44 (2011) 8644–8649, https://doi.org/10.1021/ma201070b.
[36] P.G. Frank, A. Prasher, B.T. Tuten, D. Chao, E.B. Berda, Characterization of single-chain polymer folding using size exclusion chromatography with multiple modes of detection, Appl. Petrochem. Res. 5 (2015) 9–17, https://doi.org/10.1007/s13203-014-0046-1.
[37] G. Strobl, The Physics of Polymers, Springer, Berlin Heidelberg, Berlin, Heidelberg, Heidelberg, 2007, https://doi.org/10.1007/978-3-540-68411-4.
[38] J.A. Pomposo, I. Perez-Baena, F. Lo Verso, A.J. Moreno, A. Arbe, J. Colmenero, How far are single-chain polymer nanoparticles in solution from the globular state? ACS Macro Lett. 3 (2014) 767–772, https://doi.org/10.1021/mz500354q.
[39] I. Perez-Baena, A.J. Moreno, J. Colmenero, J.A. Pomposo, Single-chain nanoparticles vs. star, hyperbranched and dendrimeric polymers: effect of the nanoscopic architecture on the flow properties of diluted solutions, Soft Matter 10 (2014) 9454–9459, https://doi.org/10.1039/c4sm01991a.
[40] G. Bryant, J.C. Thomas, Improved particle size distribution measurements using multiangle dynamic light scattering, Langmuir 11 (1995) 2480–2485, https://doi.org/10.1021/la00007a028.
[41] C.F. Bohren, D.R. Huffman, Absorption and Scattering of Light by Small Particles, Wiley-VCH Verlag GmbH, Weinheim, Germany, 1998, https://doi.org/10.1002/9783527618156.
[42] N. Ormategui, I. García, D. Padro, G. Cabañero, H.-J. Grande, I. Loinaz, Synthesis of single chain thermoresponsive polymer nanoparticles, Soft Matter 8 (2012) 734, https://doi.org/10.1039/c1sm06310c.
[43] P. Piyapakorn, T. Akagi, M. Hachisuka, T. Onishi, H. Matsuoka, M. Akashi, Structural analysis of unimer nanoparticles composed of hydrophobized poly (amino acid)s, Macromolecules 46 (2013) 6187–6194, https://doi.org/10.1021/ma4005132.
[44] K. Matsumoto, T. Terashima, T. Sugita, M. Takenaka, M. Sawamoto, Amphiphilic random copolymers with hydrophobic/hydrogen-bonding urea pendants: self-folding polymers in aqueous and organic media, Macromolecules 49 (2016) 7917–7927, https://doi.org/10.1021/acs.macromol.6b01702.
[45] G.M. ter Huurne, M.A.J. Gillissen, A.R.A. Palmans, I.K. Voets, E.W. Meijer, The coil-to-globule transition of single-chain polymeric nanoparticles with a chiral internal secondary structure, Macromolecules 48 (2015) 3949–3956, https://doi.org/10.1021/acs.macromol.5b00604.
[46] A. Sanchez-Sanchez, S. Akbari, A. Etxeberria, A. Arbe, U. Gasser, A.J. Moreno, J. Colmenero, J.A. Pomposo, "Michael" nanocarriers mimicking transient-binding disordered proteins, ACS Macro Lett. 2 (2013) 491–495, https://doi.org/10.1021/mz400173c.
[47] P.J.M. Stals, M.A.J. Gillissen, T.F.E. Paffen, T.F.A. de Greef, P. Lindner, E.W. Meijer, A.R.A. Palmans, I.K. Voets, Folding polymers with pendant hydrogen bonding motifs in water: the effect of polymer length and concentration on the shape and size of single-chain polymeric nanoparticles, Macromolecules 47 (2014) 2947–2954, https://doi.org/10.1021/ma500273g.
[48] J. Jeong, Y.-J. Lee, B. Kim, B. Kim, K.-S. Jung, H. Paik, Colored single-chain polymeric nanoparticles via intramolecular copper phthalocyanine formation, Polym. Chem. 6 (2015) 3392–3397, https://doi.org/10.1039/C4PY01559B.
[49] A.P.P. Kröger, R.J.E.A. Boonen, J.M.J. Paulusse, Well-defined single-chain polymer nanoparticles via thiol-Michael addition, Polymer 120 (2017) 119–128, https://doi.org/10.1016/j.polymer.2017.05.040.
[50] E.A. Appel, J. del Barrio, J. Dyson, L. Isaacs, O.A. Scherman, Metastable single-chain polymer nanoparticles prepared by dynamic cross-linking with nor-seco-cucurbit[10]uril, Chem. Sci. 3 (2012) 2278, https://doi.org/10.1039/c2sc20285a.
[51] E.B. Berda, E.J. Foster, E.W. Meijer, Toward controlling folding in synthetic polymers: fabricating and characterizing supramolecular single-chain nanoparticles, Macromolecules 43 (2010) 1430–1437, https://doi.org/10.1021/ma902393h.
[52] R. Gracia, M. Marradi, U. Cossío, A. Benito, A. Pérez-San Vicente, V. Gómez-Vallejo, H.-J. Grande, J. Llop, I. Loinaz, Synthesis and functionalization of dextran-based single-chain nanoparticles in aqueous media, J. Mater. Chem. B 5 (2017) 1143–1147, https://doi.org/10.1039/C6TB02773C.
[53] A.M. Hanlon, R. Chen, K.J. Rodriguez, C. Willis, J.G. Dickinson, M. Cashman, E.B. Berda, Scalable synthesis of single-chain nanoparticles under mild conditions, Macromolecules 50 (2017) 2996–3003, https://doi.org/10.1021/acs.macromol.7b00497.
[54] A.M. Hanlon, I. Martin, E.R. Bright, J. Chouinard, K.J. Rodriguez, G.E. Patenotte, E.B. Berda, Exploring structural effects in single-chain "folding" mediated by intramolecular thermal Diels–Alder chemistry, Polym. Chem. 8 (2017) 5120–5128, https://doi.org/10.1039/C7PY00320J.
[55] E.H.H. Wong, S.J. Lam, E. Nam, G.G. Qiao, Biocompatible single-chain polymeric nanoparticles via organo-catalyzed ring-opening polymerization, ACS Macro Lett. 3 (2014) 524–528, https://doi.org/10.1021/mz500225p.
[56] E.H.H. Wong, G.G. Qiao, Factors influencing the formation of single-chain polymeric nanoparticles prepared via ring-opening polymerization, Macromolecules 48 (2015) 1371–1379, https://doi.org/10.1021/ma502526c.
[57] Y. Hirai, T. Terashima, M. Takenaka, M. Sawamoto, Precision self-assembly of amphiphilic random copolymers into uniform and self-sorting nanocompartments in water, Macromolecules 49 (2016) 5084–5091, https://doi.org/10.1021/acs.macromol.6b01085.
[58] M. Shibata, M. Matsumoto, Y. Hirai, M. Takenaka, M. Sawamoto, T. Terashima, Intramolecular folding or intermolecular self-assembly of amphiphilic random copolymers: on-demand control by pendant design, Macromolecules (2018), https://doi.org/10.1021/acs.macromol.8b00570.
[59] J.É.F. Radu, L. Novak, J.F. Hartmann, N. Beheshti, A.L. Kjøniksen, B. Nyström, J. Borbély, Structural and dynamical characterization of poly-gamma-glutamic acid-based cross-linked nanoparticles, Colloid Polym. Sci. 286 (2008) 365–376, https://doi.org/10.1007/s00396-007-1776-8.
[60] T. Akagi, P. Piyapakorn, M. Akashi, Formation of unimer nanoparticles by controlling the self-association of hydrophobically modified poly(amino acid)s, Langmuir 28 (2012) 5249–5256, https://doi.org/10.1021/la205093j.
[61] K.N.R. Wuest, H. Lu, D.S. Thomas, A.S. Goldmann, M. Stenzel, C. Barner-Kowollik, Fluorescent glyco single-chain nanoparticle-decorated nanodiamonds, ACS Macro Lett. 6 (2017) 1168–1174, https://doi.org/10.1021/acsmacrolett.7b00659.
[62] C.S. Mahon, C.J. McGurk, S.M.D. Watson, M.A. Fascione, C. Sakonsinsiri, W.B. Turnbull, D.A. Fulton, Molecular recognition-mediated transformation of single-chain polymer nanoparticles into crosslinked polymer films, Angew. Chem. 56 (2017) 12913–12918, https://doi.org/10.1002/anie.201706379.
[63] A. Sanchez-Sanchez, D.A. Fulton, J.A. Pomposo, pH-responsive single-chain polymer nanoparticles utilising dynamic covalent enamine bonds, Chem. Commun. 50 (2014) 1871–1874, https://doi.org/10.1039/c3cc48733d.
[64] C. Song, L. Li, L. Dai, S. Thayumanavan, Responsive single-chain polymer nanoparticles with host–guest features, Polym. Chem. 6 (2015) 4828–4834, https://doi.org/10.1039/C5PY00600G.
[65] P.G. Frank, B.T. Tuten, A. Prasher, D. Chao, E.B. Berda, Intra-chain photodimerization of pendant anthracene units as an efficient route to single-chain nanoparticle fabrication, Macromol. Rapid Commun. 35 (2014) 249–253, https://doi.org/10.1002/marc.201300677.
[66] J. He, L. Tremblay, S. Lacelle, Y. Zhao, Preparation of polymer single chain nanoparticles using intramolecular photodimerization of coumarin, Soft Matter 7 (2011) 2380–2386, https://doi.org/10.1039/c0sm01383h.
[67] J. Willenbacher, B.V.K.J. Schmidt, D. Schulze-Sünninghausen, O. Altintas, B. Luy, G. Delaittre, C. Barner-Kowollik, Reversible single-chain selective point folding via cyclodextrin driven host–guest chemistry in water, Chem. Commun. 50 (2014) 7056–7059, https://doi.org/10.1039/c4cc03218g.
[68] F. Wang, H. Pu, X. Che, Voltage-responsive single-chain polymer nanoparticles via host–guest interaction, Chem. Commun. 52 (2016) 3516–3519, https://doi.org/10.1039/C5CC09984F.
[69] C. Heiler, J.T. Offenloch, E. Blasco, C. Barner-Kowollik, Photochemically induced folding of single chain polymer nanoparticles in water, ACS Macro Lett. 6 (2017) 56–61, https://doi.org/10.1021/acsmacrolett.6b00858.
[70] S.K. Hamilton, E. Harth, Molecular dendritic transporter nanoparticle vectors provide efficient intracellular delivery of peptides, ACS Nano 3 (2009) 402–410, https://doi.org/10.1021/nn800679z.
[71] G. Qian, B. Zhu, Y. Wang, S. Deng, A. Hu, Size-tunable polymeric nanoreactors for one-pot synthesis and encapsulation of quantum dots, Macromol. Rapid Commun. 33 (2012) 1393–1398, https://doi.org/10.1002/marc.201200199.
[72] C.T. Adkins, J.N. Dobish, S. Brown, E. Harth, Water-soluble semiconducting nanoparticles for imaging, ACS Macro Lett. 2 (2013) 710–714, https://doi.org/10.1021/mz400370f.

[73] Y. Bai, H. Xing, G.A. Vincil, J. Lee, E.J. Henderson, Y. Lu, N.G. Lemcoff, S.C. Zimmerman, Practical synthesis of water-soluble organic nanoparticles with a single reactive group and a functional carrier scaffold, Chem. Sci. 5 (2014) 2862–2868, https://doi.org/10.1039/C4SC00700J.
[74] Y. Bai, H. Xing, P. Wu, X. Feng, K. Hwang, J.M. Lee, X.Y. Phang, Y. Lu, S.C. Zimmerman, Chemical control over cellular uptake of organic nanoparticles by fine tuning surface functional groups, ACS Nano 9 (2015) 10227–10236, https://doi.org/10.1021/acsnano.5b03909.
[75] Y. Li, Y. Bai, N. Zheng, Y. Liu, G.A. Vincil, B. Pedretti, J. Cheng, S.C. Zimmerman, Crosslinked dendronized polyols as a general approach to brighter and more stable fluorophores, Chem. Commun. 52 (2016) 3781–3784, https://doi.org/10.1039/C5CC09430E.
[76] A.P.P. Kröger, N.M. Hamelmann, A. Juan, S. Lindhoud, J.M.J. Paulusse, Biocompatible Single-Chain Polymer Nanoparticles for Drug Delivery – A Dual Approach, (2018).
[77] A.B. Benito, M.K. Aiertza, M. Marradi, L. Gil-Iceta, T. Shekhter Zahavi, B. Szczupak, M. Jiménez-González, T. Reese, E. Scanziani, L. Passoni, M. Matteoli, M. De Maglie, A. Orenstein, M. Oron-Herman, G. Kostenich, L. Buzhansky, E. Gazit, H.J. Grande, V. Gómez-Vallejo, J. Llop, I. Loinaz, Functional single-chain polymer nanoparticles: targeting and imaging pancreatic tumors in vivo, Biomacromolecules 17 (2016) 3213–3221, https://doi.org/10.1021/acs.biomac.6b00941.
[78] Y. Zhang, H. Zhao, Surface-tunable colloidal particles stabilized by mono-tethered single-chain nanoparticles, Polymer 64 (2015) 277–284, https://doi.org/10.1016/j.polymer.2015.02.005.
[79] J. Willenbacher, K.N.R. Wuest, J.O. Mueller, M. Kaupp, H. Wagenknecht, C. Barner-Kowollik, Photochemical design of functional fluorescent single-chain nanoparticles, ACS Macro Lett. 3 (2014) 574–579, https://doi.org/10.1021/mz500292e.
[80] R. Gracia, M. Marradi, G. Salerno, R. Pérez-Nicado, A. Pérez-San Vicente, D. Dupin, J. Rodriguez, I. Loinaz, F. Chiodo, C. Nativi, Biocompatible single-chain polymer nanoparticles loaded with an antigen mimetic as potential anticancer vaccine, ACS Macro. Lett. (2018) 196–200, https://doi.org/10.1021/acsmacrolett.8b00052.
[81] E.A. Appel, J. Dyson, J. del Barrio, Z. Walsh, O.A. Scherman, Formation of single-chain polymer nanoparticles in water through host-guest interactions, Angew. Chem. 51 (2012) 4185–4189, https://doi.org/10.1002/anie.201108659.
[82] Z. Zhu, N. Xu, Q. Yu, L. Guo, H. Cao, X. Lu, Y. Cai, Construction and self-assembly of single-chain polymer nanoparticles via coordination association and electrostatic repulsion in water, Macromol. Rapid Commun. 36 (2015) 1521–1527, https://doi.org/10.1002/marc.201500281.
[83] H. Cao, Z. Cui, P. Gao, Y. Ding, X. Zhu, X. Lu, Y. Cai, Metal-folded single-chain nanoparticle: nanoclusters and self-assembled reduction-responsive sub-5-nm discrete subdomains, Macromol. Rapid Commun. 38 (2017) 1700269, https://doi.org/10.1002/marc.201700269.
[84] Z. Cui, H. Cao, Y. Ding, P. Gao, X. Lu, Y. Cai, Compartmentalization of an ABC triblock copolymer single-chain nanoparticle via coordination-driven orthogonal self-assembly, Polym. Chem. 8 (2017) 3755–3763, https://doi.org/10.1039/C7PY00582B.
[85] Y. Bai, X. Feng, H. Xing, Y. Xu, B.K. Kim, N. Baig, T. Zhou, A.A. Gewirth, Y. Lu, E. Oldfield, S.C. Zimmerman, A highly efficient single-chain metal-organic nanoparticle catalyst for alkyne-azide “click” reactions in water and in cells, J. Am. Chem. Soc. 138 (2016) 11077–11080, https://doi.org/10.1021/jacs.6b04477.
[86] F. Wang, H. Pu, M. Jin, D. Wan, Supramolecular nanoparticles via single-chain folding driven by ferrous ions, Macromol. Rapid Commun. 37 (2016) 330–336, https://doi.org/10.1002/marc.201500616.
[87] R. Lambert, A.-L. Wirotius, D. Taton, Intramolecular quaternization as folding strategy for the synthesis of catalytically active imidazolium-based single chain nanoparticles, ACS Macro Lett. 6 (2017) 489–494, https://doi.org/10.1021/acsmacrolett.7b00161.
[88] J. Zhang, G. Gody, M. Hartlieb, S. Catrouillet, J. Moffat, S. Perrier, Synthesis of sequence-controlled multiblock single chain nanoparticles by a stepwise folding–chain extension–folding process, Macromolecules 49 (2016) 8933–8942, https://doi.org/10.1021/acs.macromol.6b01962.
[89] J.-H. Ryu, R.T. Chacko, S. Jiwpanich, S. Bickerton, R.P. Babu, S. Thayumanavan, Self-cross-linked polymer nanogels: a versatile nanoscopic drug delivery platform, J. Am. Chem. Soc. 132 (2010) 17227–17235, https://doi.org/10.1021/ja1069932.
[90] Y. Morishima, S. Nomura, T. Ikeda, M. Seki, M. Kamachi, Characterization of unimolecular micelles of random copolymers of sodium 2-(acrylamido)-2-methylpropanesulfonate and methacrylamides bearing bulky hydrophobic substituents, Macromolecules 28 (1995) 2874–2881, https://doi.org/10.1021/ma00112a037.
[91] T. Terashima, T. Sugita, K. Fukae, M. Sawamoto, Synthesis and single-chain folding of amphiphilic random copolymers in water, Macromolecules 47 (2014) 589–600, https://doi.org/10.1021/ma402355v.
[92] Y. Koda, T. Terashima, M. Sawamoto, Multimode self-folding polymers via reversible and thermoresponsive self-assembly of amphiphilic/fluorous random copolymers, Macromolecules 49 (2016) 4534–4543, https://doi.org/10.1021/acs.macromol.6b00998.
[93] Y. Zhang, R. Tan, M. Gao, P. Hao, D. Yin, Bio-inspired single-chain polymeric nanoparticles containing a chiral salen Ti IV complex for highly enantioselective sulfoxidation in water, Green Chem. 19 (2017) 1182–1193, https://doi.org/10.1039/C6GC02743A.
[94] C. Riddles, W. Zhao, H.-J. Hu, M. Chen, M.R. Van De Mark, Self-assembly of water insoluble polymers into colloidal unimolecular polymer (CUP) particles of 3–9 nm, Polymer 55 (2014) 48–57, https://doi.org/10.1016/j.polymer.2013.11.014.
[95] A.M. Natu, M. Wiggins, M.R. Van De Mark, Synthesis and characterization of cationic colloidal unimolecular polymer (CUP) particles, Colloid Polym. Sci. 293 (2015) 1191–1204, https://doi.org/10.1007/s00396-015-3508-9.
[96] J.K. Mistry, M.R. Van De Mark, Aziridine cure of acrylic colloidal unimolecular polymers (CUPs), J. Coat. Technol. Res. 10 (2013) 453–463, https://doi.org/10.1007/s11998-013-9489-z.
[97] S. Yusa, A. Sakakibara, T. Yamamoto, Y. Morishima, Reversible pH-induced formation and disruption of unimolecular micelles of an amphiphilic polyelectrolyte, Macromolecules 35 (2002) 5243–5249, https://doi.org/10.1021/ma0200930.
[98] A. Bartolini, P. Tempesti, C. Resta, D. Berti, J. Smets, Y.G. Aouad, P. Baglioni, Poly (ethylene glycol)-graft-poly(vinyl acetate) single-chain nanoparticles for the encapsulation of small molecules, Phys. Chem. Chem. Phys. 19 (2017) 4553–4559, https://doi.org/10.1039/C6CP07967A.
[99] J. Liang, J.J. Struckhoff, P.D. Hamilton, N. Ravi, Preparation and characterization of biomimetic β-lens crystallins using single-chain polymeric nanoparticles, Langmuir 33 (2017) 7660–7668, https://doi.org/10.1021/acs.langmuir.7b01290.
[100] A. Sanchez-Sanchez, A. Arbe, J. Kohlbrecher, J. Colmenero, J.A. Pomposo, Efficient synthesis of single-chain globules mimicking the morphology and polymerase activity of metalloenzymes, Macromol. Rapid Commun. 36 (2015) 1592–1597, https://doi.org/10.1002/marc.201500252.
[101] S. Basasoro, M. González-Burgos, A.J. Moreno, F. Lo Verso, A. Arbe, J. Colmenero, J.A. Pomposo, A solvent-based strategy for tuning the internal structure of metallo-folded single-chain nanoparticles, Macromol. Rapid Commun. 37 (2016) 1060–1065, https://doi.org/10.1002/marc.201600139.
[102] C.-C. Cheng, F.-C. Chang, H.-C. Yen, D.-J. Lee, C.-W. Chiu, Z. Xin, Supramolecular assembly mediates the formation of single-chain polymeric nanoparticles, ACS Macro Lett. 4 (2015) 1184–1188, https://doi.org/10.1021/acsmacrolett.5b00556.
[103] C.-C. Cheng, D.-J. Lee, Z.-S. Liao, J.-J. Huang, Stimuli-responsive single-chain polymeric nanoparticles towards the development of efficient drug delivery systems, Polym. Chem. 7 (2016) 6164–6169, https://doi.org/10.1039/C6PY01623E.
[104] Y. Liu, T. Pauloehrl, S.I. Presolski, L. Albertazzi, A.R.A. Palmans, E.W. Meijer, Modular synthetic platform for the construction of functional single-chain polymeric nanoparticles: from aqueous catalysis to photosensitization, J. Am. Chem. Soc. 137 (2015) 13096–13105, https://doi.org/10.1021/jacs.5b08299.
[105] E. Huerta, P.J.M. Stals, E.W. Meijer, A.R.A. Palmans, Consequences of folding a water-soluble polymer around an organocatalyst, Angew. Chem. 52 (2013) 2906–2910, https://doi.org/10.1002/anie.201207123.
[106] M. Artar, T. Terashima, M. Sawamoto, E.W. Meijer, A.R.A. Palmans, Understanding the catalytic activity of single-chain polymeric nanoparticles in water, J. Polym. Sci. Part A Polym. Chem. 52 (2014) 12–20, https://doi.org/10.1002/pola.26970.
[107] M. Artar, Single chain polymeric nanoparticles as selective hydrophobic reaction spaces in water, ACS Macro Lett. 4 (2015) 1099–1103, https://doi.org/10.1021/acsmacrolett.5b00652.
[108] P.J.M. Stals, C.-Y. Cheng, L. van Beek, A.C. Wauters, A.R.A. Palmans, S. Han, E.W. Meijer, Surface water retardation around single-chain polymeric nanoparticles: critical for catalytic function? Chem. Sci. 7 (2016) 2011–2015, https://doi.org/10.1039/C5SC02319J.
[109] Y. Liu, S. Pujals, P.J.M. Stals, T. Paulöhrl, S.I. Presolski, E.W. Meijer, L. Albertazzi, A.R.A. Palmans, Catalytically active single-chain polymeric nanoparticles: exploring their functions in complex biological media, J. Am. Chem. Soc. (2018), https://doi.org/10.1021/jacs.8b00122.
[110] M. Chen, C. Riddles, M.R. Van De Mark, Gel point behavior of colloidal unimolecular polymer (CUP) particles, Colloid Polym. Sci. 291 (2013) 2893–2901, https://doi.org/10.1007/s00396-013-3034-6.
[111] M. Chen, C. Riddles, M.R. Van De Mark, Electroviscous contribution to the rheology of colloidal unimolecular polymer (CUP) particles in water, Langmuir 29 (2013) 14034–14043, https://doi.org/10.1021/la4026552.
[112] P. Theato, H.A. Klok, Functional Polymers by Post-Polymerization Modification, Wiley-VCH Verlag GmbH & Co. KGaA, Weinheim, Germany, 2012, https://doi.org/10.1002/9783527655427.
[113] Y. Koda, T. Terashima, M. Sawamoto, H.D. Maynard, Amphiphilic/fluorous random copolymers as a new class of non-cytotoxic polymeric materials for protein conjugation, Polym. Chem. 6 (2015) 240–247, https://doi.org/10.1039/C4PY01346H.
[114] M. Eberhardt, R. Mruk, R. Zentel, P. Theato, Synthesis of pentafluorophenyl(meth) acrylate polymers: new precursor polymers for the synthesis of multifunctional materials, Eur. Polym. J. 41 (2005) 1569–1575, https://doi.org/10.1016/j.eurpolymj.2005.01.025.
[115] J. De-La-Cuesta, E. González, J.A. Pomposo, Advances in fluorescent single-chain nanoparticles, Molecules 22 (2017) 1819, https://doi.org/10.3390/molecules22111819.
[116] E.J. Foster, E.B. Berda, E.W. Meijer, Tuning the size of supramolecular single-chain polymer nanoparticles, J. Polym. Sci. Part A Polym. Chem. 49 (2011) 118–126, https://doi.org/10.1002/pola.24426.
[117] A.J. Moreno, P. Bacova, F. Lo Verso, A. Arbe, J. Colmenero, J.A. Pomposo, Effect of chain stiffness on the structure of single-chain polymer nanoparticles, J. Phys. Condens. Matter 30 (2018) 034001, , https://doi.org/10.1088/1361-648X/aa9f5c.
[118] K. Watanabe, R. Tanaka, K. Takada, M.-J. Kim, J.-S. Lee, K. Tajima, T. Isono, T. Satoh, Intramolecular olefin metathesis as a robust tool to synthesize single-chain nanoparticles in a size-controlled manner, Polym. Chem. 7 (2016) 4782–4792, https://doi.org/10.1039/C6PY00795C.
[119] A.J. Moreno, F. Lo Verso, A. Sanchez-Sanchez, A. Arbe, J. Colmenero, J.A. Pomposo, Advantages of orthogonal folding of single polymer chains to soft

nanoparticles, Macromolecules 46 (2013) 9748–9759, https://doi.org/10.1021/ma4021399.
[120] F. Lo Verso, J.A. Pomposo, J. Colmenero, A.J. Moreno, Multi-orthogonal folding of single polymer chains into soft nanoparticles, Soft Matter 10 (2014) 4813–4821, https://doi.org/10.1039/C4SM00459K.
[121] I. Perez-Baena, I. Asenjo-Sanz, A. Arbe, A.J. Moreno, F. Lo Verso, J. Colmenero, J.A. Pomposo, Efficient route to compact single-chain nanoparticles: photo-activated synthesis via thiol–yne coupling reaction, Macromolecules 47 (2014) 8270–8280, https://doi.org/10.1021/ma5017133.
[122] G.M. ter Huurne, L.N.J. de Windt, Y. Liu, E.W. Meijer, I.K. Voets, A.R.A. Palmans, Improving the folding of supramolecular copolymers by controlling the assembly pathway complexity, Macromolecules 50 (2017) 8562–8569, https://doi.org/10.1021/acs.macromol.7b01769.
[123] H. Yamamoto, Y. Morishima, Effect of hydrophobe content on intra- and inter-polymer self-associations of hydrophobically modified poly(sodium 2-(acrylamido)-2-methylpropanesulfonate) in water, Macromolecules 32 (1999) 7469–7475, https://doi.org/10.1021/ma9907791.
[124] P.J.M. Stals, M.A.J. Gillissen, R. Nicolaÿ, A.R.A. Palmans, E.W. Meijer, B. Charleux, J.K.L. Lowe, M.J.A. van Luyn, The balance between intramolecular hydrogen bonding, polymer solubility and rigidity in single-chain polymeric nanoparticles, Polym. Chem. 4 (2013) 2584, https://doi.org/10.1039/c3py00094j.
[125] M. Seo, J.B. Beck, J.M.J. Paulusse, C.J. Hawker, S.Y. Kim, Polymeric nanoparticles via noncovalent cross-linking of linear chains, Macromolecules 41 (2008) 6413–6418, https://doi.org/10.1021/ma8009678.
[126] F. Lo Verso, J.A. Pomposo, J. Colmenero, A.J. Moreno, Simulation guided design of globular single-chain nanoparticles by tuning the solvent quality, Soft Matter 11 (2015) 1369–1375, https://doi.org/10.1039/C4SM02475C.
[127] Y. Gao, D. Zhou, T. Zhao, X. Wei, S. McMahon, J. O'Keeffe Ahern, W. Wang, U. Greiser, B.J. Rodriguez, Intramolecular cyclization dominating homo-polymerization of multivinyl monomers toward single-chain cyclized/knotted polymeric nanoparticles, Macromolecules 48 (2015) 6882–6889, https://doi.org/10.1021/acs.macromol.5b01549.
[128] L. Cutlar, Y. Gao, A. Aied, U. Greiser, E.M. Murauer, D. Zhou, W. Wang, A knot polymer mediated non-viral gene transfection for skin cells, Biomater. Sci. 4 (2016) 92–95, https://doi.org/10.1039/C5BM00216H.
[129] Y. Gao, V.I. Böhmer, D. Zhou, T. Zhao, W. Wang, J.M.J. Paulusse, Main-chain degradable single-chain cyclized polymers as gene delivery vectors, J. Control. Release 244 (2016) 375–383, https://doi.org/10.1016/j.jconrel.2016.07.046.
[130] Y. Gao, B. Newland, D. Zhou, K. Matyjaszewski, W. Wang, Controlled polymerization of multivinyl monomers: formation of cyclized/knotted single-chain polymer architectures, Angew. Chem. Int. Ed. 56 (2017) 450–460, https://doi.org/10.1002/anie.201608786.
[131] E. Blasco, B.T. Tuten, H. Frisch, A. Lederer, C. Barner-Kowollik, Characterizing single chain nanoparticles (SCNPs): a critical survey, Polym. Chem. 8 (2017) 5845–5851, https://doi.org/10.1039/C7PY01278K.
[132] Y. Williams, A. Sukhanova, M. Nowostawska, A.M. Davies, S. Mitchell, V. Oleinikov, Y. Gun'ko, I. Nabiev, D. Kelleher, Y. Volkov, Probing cell-type-specific intracellular nanoscale barriers using size-tuned quantum dots, Small 5 (2009) 2581–2588, https://doi.org/10.1002/smll.200900744.
[133] R. Agarwal, V. Singh, P. Jurney, L. Shi, S.V. Sreenivasan, K. Roy, Mammalian cells preferentially internalize hydrogel nanodiscs over nanorods and use shape-specific uptake mechanisms, Proc. Natl. Acad. Sci. 110 (2013) 17247–17252, https://doi.org/10.1073/pnas.1305000110.
[134] J. Sun, L. Zhang, J. Wang, Q. Feng, D. Liu, Q. Yin, D. Xu, Y. Wei, B. Ding, X. Shi, X. Jiang, Tunable rigidity of (polymeric core)-(lipid shell) nanoparticles for regulated cellular uptake, Adv. Mater. 27 (2015) 1402–1407, https://doi.org/10.1002/adma.201404788.
[135] A.H. Bahrami, M. Raatz, J. Agudo-Canalejo, R. Michel, E.M. Curtis, C.K. Hall, M. Gradzielski, R. Lipowsky, T.R. Weikl, Wrapping of nanoparticles by membranes, Adv. Colloid Interf. Sci. 208 (2014) 214–224, https://doi.org/10.1016/J.CIS.2014.02.012.
[136] D. Wang, R.J. Nap, I. Lagzi, B. Kowalczyk, S. Han, B.A. Grzybowski, I. Szleifer, How and why nanoparticle's curvature regulates the apparent pKa of the coating ligands, J. Am. Chem. Soc. 133 (2011) 2192–2197, https://doi.org/10.1021/ja108154a.
[137] M. Longmire, P.L. Choyke, H. Kobayashi, Clearance properties of nano-sized particles and molecules as imaging agents: considerations and caveats, Nanomedicine 3 (2008) 703–717, https://doi.org/10.2217/17435889.3.5.703.
[138] F. Joux, P. Lebaron, Use of fluorescent probes to assess physiological functions of bacteriaat single-cell level, Microbes Infect. 2 (2000) 1523–1535, https://doi.org/10.1016/S1286-4579(00)01307-1.
[139] M.A. Dobrovolskaia, J.D. Clogston, B.W. Neun, J.B. Hall, A.K. Patri, S.E. McNeil, Method for analysis of nanoparticle hemolytic properties in vitro, Nano Lett. 8 (2008) 2180–2187, https://doi.org/10.1021/nl0805615.
[140] T.-K. Nguyen, S.J. Lam, K.K.K. Ho, N. Kumar, G.G. Qiao, S. Egan, C. Boyer, E.H.H. Wong, Rational design of single-chain polymeric nanoparticles that kill planktonic and biofilm bacteria, ACS Infect. Dis. (2017), https://doi.org/10.1021/acsinfecdis.6b00203.
[141] A. Latorre-Sánchez, J.A. Pomposo, A simple, fast and highly sensitive colorimetric detection of zein in aqueous ethanol via zein–pyridine–gold interactions, Chem. Commun. 51 (2015) 15736–15738, https://doi.org/10.1039/C5CC06083D.
[142] M.A.J. Gillissen, I.K. Voets, E.W. Meijer, A.R.A. Palmans, Single chain polymeric nanoparticles as compartmentalised sensors for metal ions, Polym. Chem. 3 (2012) 3166, https://doi.org/10.1039/c2py20350b.
[143] A. Sanchez-Sanchez, S. Akbari, A.J. Moreno, F. Lo Verso, A. Arbe, J. Colmenero, J.A. Pomposo, Design and preparation of single-chain nanocarriers mimicking disordered proteins for combined delivery of dermal bioactive cargos, Macromol. Rapid Commun. 34 (2013) 1681–1686, https://doi.org/10.1002/marc.201300562.
[144] K. Morishima, K. Terao, T. Sato, Structural analysis of hydrophobe-uptake micelle of an amphiphilic alternating copolymer in aqueous solution, Langmuir 32 (2016) 7875–7881, https://doi.org/10.1021/acs.langmuir.6b01480.
[145] R. Deans, F. Ilhan, V.M. Rotello, Recognition-mediated unfolding of a self-assembled polymeric globule, Macromolecules 32 (1999) 4956–4960, https://doi.org/10.1021/ma990735s.
[146] T.H. Galow, F. Ilhan, G. Cooke, V.M. Rotello, Recognition and encapsulation of an electroactive guest within a dynamically folded polymer, J. Am. Chem. Soc. 122 (2000) 3595–3598, https://doi.org/10.1021/ja993735g.
[147] L.L. Lao, N.A. Peppas, F.Y.C. Boey, S.S. Venkatraman, Modeling of drug release from bulk-degrading polymers, Int. J. Pharm. 418 (2011) 28–41, https://doi.org/10.1016/j.ijpharm.2010.12.020.
[148] Y. Koda, T. Terashima, H.D. Maynard, M. Sawamoto, Protein storage with perfluorinated PEG compartments in a hydrofluorocarbon solvent, Polym. Chem. 7 (2016) 6694–6698, https://doi.org/10.1039/C6PY01333C.
[149] D. Mandracchia, A.P. Piccionello, G. Pitarresi, A. Pace, S. Buscemi, G. Giammona, Fluoropolymer based on a polyaspartamide containing 1,2,4-oxadiazole units: a potential artificial oxygen (O_2) carrier, Macromol. Biosci. 7 (2007) 836–845, https://doi.org/10.1002/mabi.200600266.
[150] V.N. Mochalin, O. Shenderova, D. Ho, Y. Gogotsi, The properties and applications of nanodiamonds, Nat. Nanotechnol. 7 (2012) 11–23, https://doi.org/10.1038/nnano.2011.209.
[151] J. Li, F. Yu, Y. Chen, D. Oupický, Polymeric drugs: advances in the development of pharmacologically active polymers, J. Control. Release 219 (2015) 369–382, https://doi.org/10.1016/j.jconrel.2015.09.043.
[152] E.F. Connor, I. Lees, D. Maclean, Polymers as drugs-advances in therapeutic applications of polymer binding agents, J. Polym. Sci. Part A Polym. Chem. 55 (2017) 3146–3157, https://doi.org/10.1002/pola.28703.
[153] K.P. Johnson, B.R. Brooks, J.A. Cohen, C.C. Ford, J. Goldstein, R.P. Lisak, L.W. Myers, H.S. Panitch, J.W. Rose, R.B. Schiffer, T. Vollmer, L.P. Weiner, J.S. Wolinsky, Extended use of glatiramer acetate (Copaxone) is well tolerated and maintains its clinical effect on multiple sclerosis relapse rate and degree of disability, Neurology 50 (1998) 701–708, https://doi.org/10.1212/WNL.50.3.701.
[154] J. Liu, G. Feng, R. Liu, N. Tomczak, L. Ma, G.G. Gurzadyan, B. Liu, Bright quantum-dot-sized single-chain conjugated polyelectrolyte nanoparticles: synthesis, characterization and application for specific extracellular labeling and imaging, Small 10 (2014) 3110–3118, https://doi.org/10.1002/smll.201303505.
[155] B. Zhu, S. Sun, Y. Wang, S. Deng, G. Qian, M. Wang, A. Hu, Preparation of carbon nanodots from single chain polymeric nanoparticles and theoretical investigation of the photoluminescence mechanism, J. Mater. Chem. C 1 (2013) 580–586, https://doi.org/10.1039/C2TC00140C.
[156] H. Xing, Y. Bai, Y. Bai, L.H. Tan, J. Tao, B. Pedretti, G.A. Vincil, Y. Lu, S.C. Zimmerman, Bottom-up strategy to prepare nanoparticles with a single DNA strand, J. Am. Chem. Soc. 139 (2017) 3623–3626, https://doi.org/10.1021/jacs.7b00065.
[157] X. Michalet, F.F. Pinaud, L.A. Bentolila, J.M. Tsay, S. Doose, J.J. Li, G. Sundaresan, A.M. Wu, S.S. Gambhir, S. Weiss, Quantum dots for live cells, in vivo imaging, and diagnostics, Science 307 (2005) 538–544, https://doi.org/10.1126/science.1104274.
[158] I.L. Medintz, H. Mattoussi, A.R. Clapp, Potential clinical applications of quantum dots, Int. J. Nanomedicine 3 (2008) 151–167 http://www.ncbi.nlm.nih.gov/pubmed/18686776.
[159] L.E. Cole, R.D. Ross, J.M. Tilley, T. Vargo-Gogola, R.K. Roeder, Gold nanoparticles as contrast agents in X-ray imaging and computed tomography, Nanomedicine 10 (2015) 321–341, https://doi.org/10.2217/nnm.14.171.
[160] W.A. Braunecker, K. Matyjaszewski, Controlled/living radical polymerization: features, developments, and perspectives, Prog. Polym. Sci. 32 (2007) 93–146, https://doi.org/10.1016/j.progpolymsci.2006.11.002.
[161] N. Badi, J.-F. Lutz, Sequence control in polymer synthesis, Chem. Soc. Rev. 38 (2009) 3383, https://doi.org/10.1039/b806413j.
[162] J. Vandenbergh, G. Reekmans, P. Adriaensens, T. Junkers, Synthesis of sequence controlled acrylate oligomers via consecutive RAFT monomer additions, Chem. Commun. 49 (2013) 10358, https://doi.org/10.1039/c3cc45994b.
[163] W.R. Gutekunst, C.J. Hawker, A general approach to sequence-controlled polymers using macrocyclic ring opening metathesis polymerization, J. Am. Chem. Soc. 137 (2015) 8038–8041, https://doi.org/10.1021/jacs.5b04940.
[164] S.C. Solleder, D. Zengel, K.S. Wetzel, M.A.R. Meier, A scalable and high-yield strategy for the synthesis of sequence-defined macromolecules, Angew. Chem. Int. Ed. 55 (2016) 1204–1207, https://doi.org/10.1002/anie.201509398.
[165] Y. Hibi, M. Ouchi, M. Sawamoto, A strategy for sequence control in vinyl polymers via iterative controlled radical cyclization, Nat. Commun. 7 (2016) 11064, https://doi.org/10.1038/ncomms11064.
[166] B.V.K.J. Schmidt, N. Fechler, J. Falkenhagen, J.-F. Lutz, Controlled folding of synthetic polymer chains through the formation of positionable covalent bridges, Nat. Chem. 3 (2011) 234–238, https://doi.org/10.1038/nchem.964.
[167] O. Shishkan, M. Zamfir, M.A. Gauthier, H.G. Börner, J.-F. Lutz, Complex single-chain polymer topologies locked by positionable twin disulfide cyclic bridges, Chem. Commun. 50 (2014) 1570–1572, https://doi.org/10.1039/c3cc47807f.
[168] J.P. Cole, J.J. Lessard, K.J. Rodriguez, A.M. Hanlon, E.K. Reville, J.P. Mancinelli, E.B. Berda, Single-chain nanoparticles containing sequence-defined segments: using primary structure control to promote secondary and tertiary structures in synthetic protein mimics, Polym. Chem. 8 (2017) 5829–5835, https://doi.org/10.1039/C7PY01133D.

[169] E. Huerta, B. van Genabeek, P.J.M. Stals, E.W. Meijer, A.R.A. Palmans, A modular approach to introduce function into single-chain polymeric nanoparticles, Macromol. Rapid Commun. 35 (2014) 1320–1325, https://doi.org/10.1002/marc.201400213.
[170] A. Latorre-Sánchez, J.A. Pomposo, Recent bioinspired applications of single-chain nanoparticles, Polym. Int. 65 (2016) 855–860, https://doi.org/10.1002/pi.5078.
[171] O. Altintas, E. Lejeune, P. Gerstel, C. Barner-Kowollik, Bioinspired dual self-folding of single polymer chains via reversible hydrogen bonding, Polym. Chem. 3 (2012) 640, https://doi.org/10.1039/c1py00392e.
[172] O. Altintas, P. Krolla-Sidenstein, H. Gliemann, C. Barner-Kowollik, Single-chain folding of diblock copolymers driven by orthogonal H-donor and acceptor units, Macromolecules 47 (2014) 5877–5888, https://doi.org/10.1021/ma501186k.
[173] T.S. Fischer, D. Schulze-Sünninghausen, B. Luy, O. Altintas, C. Barner-Kowollik, Stepwise unfolding of single-chain nanoparticles by chemically triggered gates, Angew. Chem. 55 (2016) 11276–11280, https://doi.org/10.1002/anie.201602894.
[174] O. Altintas, M. Artar, G. ter Huurne, I.K. Voets, A.R.A. Palmans, C. Barner-Kowollik, E.W. Meijer, Design and synthesis of triblock copolymers for creating complex secondary structures by orthogonal self-assembly, Macromolecules 48 (2015) 8921–8932, https://doi.org/10.1021/acs.macromol.5b01990.
[175] D. Chao, X. Jia, B.T. Tuten, C. Wang, E.B. Berda, Controlled folding of a novel electroactive polyolefin via multiple sequential orthogonal intra-chain interactions, Chem. Commun. 49 (2013) 4178–4180, https://doi.org/10.1039/C2CC37157J.
[176] R.K. Roy, J.-F. Lutz, Compartmentalization of single polymer chains by stepwise intramolecular cross-linking of sequence-controlled macromolecules, J. Am. Chem. Soc. 136 (2014) 12888–12891, https://doi.org/10.1021/ja507889x.
[177] C.A. Tooley, S. Pazicni, E.B. Berda, Toward a tunable synthetic [FeFe] hydrogenase mimic: single-chain nanoparticles functionalized with a single diiron cluster, Polym. Chem. 6 (2015) 7646–7651, https://doi.org/10.1039/C5PY01196E.
[178] I. Perez-Baena, F. Barroso-Bujans, U. Gasser, A. Arbe, A.J. Moreno, J. Colmenero, J.A. Pomposo, Endowing single-chain polymer nanoparticles with enzyme-mimetic activity, ACS Macro Lett. 2 (2013) 775–779, https://doi.org/10.1021/mz4003744.
[179] J. Rubio-Cervilla, E. González, J.A. Pomposo, Advances in single-chain nanoparticles for catalysis applications, Nano 7 (2017) 341, https://doi.org/10.3390/nano7100341.
[180] J.P. Cole, A.M. Hanlon, K.J. Rodriguez, E.B. Berda, Protein-like structure and activity in synthetic polymers, J. Polym. Sci. Part A Polym. Chem. 55 (2017) 191–206, https://doi.org/10.1002/pola.28378.
[181] K.J. Rodriguez, A.M. Hanlon, C.K. Lyon, J.P. Cole, B.T. Tuten, C.A. Tooley, E.B. Berda, S. Pazicni, Porphyrin-cored polymer nanoparticles: macromolecular models for heme iron coordination, Inorg. Chem. 55 (2016) 9493–9496, https://doi.org/10.1021/acs.inorgchem.6b01113.